ACS APPLIED MATERIALS & INTERFACES

www.acsami.org

Research Article

Selective Promotion of Adhesion of *Shewanella oneidensis* on Mannose-Decorated Glycopolymer Surfaces

Thomas D. Young, Walter T. Liau, Calvin K. Lee, Michael Mellody, Gerard C. L. Wong, Andrea M. Kasko, and Paul S. Weiss*

Cite This: *ACS Appl. Mater. Interfaces* 2020, 12, 35767–35781

Read Online

ACCESS | Metrics & More | Article Recommendations | Supporting Information

ABSTRACT: Using glycopolymer surfaces, we have stimulated *Shewanella oneidensis* bacterial colonization and induced where the bacteria attach on a molecular pattern. When adherent bacteria were rinsed with methyl α-D-mannopyranoside, the glycopolymer-functionalized surfaces retained more cells than self-assembled monolayers terminated by a single mannose unit. These results suggest that the three-dimensional multivalency of the glycopolymers both promotes and retains bacterial attachment. When the methyl α-D-mannopyranoside competitor was codeposited with the cell culture, however, the mannose-based polymer was not significantly different from bare gold surfaces. The necessity for equilibration between methyl α-D-mannopyranoside and the cell culture to remove the enhancement suggests that the retention of cells on glycopolymer surfaces is kinetically controlled and is not a thermodynamic result of the cluster glycoside effect. The MshA lectin appears to facilitate the improved adhesion observed. Our findings that the surfaces studied here can induce stable initial attachment and influence the ratio of bacterial strains on the surface may be applied to harness useful microbial communities.

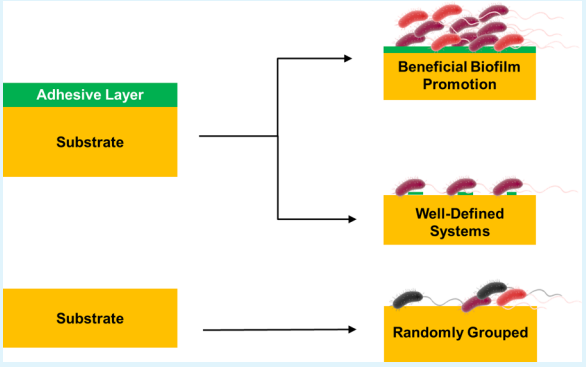

KEYWORDS: *Shewanella, glycopolymer, adhesion, biofilm, mannose, electrode, cell density, patterning*

INTRODUCTION

Interactions of microorganisms and surfaces are fundamental components of their lives and activity. Surface sensing and adhesion to surfaces by planktonic cells are the first steps of surface colonization and formation of microbial biofilms; a biofilm is a collection of microbes and the surrounding material that symbiotically forms on surfaces. As such, understanding adhesion, surface sensing, and colonization are crucial to understanding biofilms, which are often the natural and scientifically relevant state of bacteria and other microbes.[1] In addition to providing physical connections, surface interactions by bacteria produce cellular responses that influence colonization behaviors, including modulation of motility appendages and production of secreted adhesives.[2] Colonization can be affected by bacterial interactions with surfaces, even when the microbe is no longer in close proximity.[3] Where a robust biofilm and microbial colony are desirable, irreversible attachment of cells after surface interaction is essential.[4] Unstable biofilms may disperse or become nonactive, particularly in the event of temporary nutrient insufficiency.[5]

There are several examples of beneficial types of microbial biofilms. Microbes, frequently bacteria, are used in biocatalytic systems, which exploit the microbe's metabolism to perform anodic or cathodic processes. Anabolic processes harnessed by microbial chassis can produce high-value chemicals by biosynthesis,[6−9] and catabolic processes can capture energy or remove unwanted materials from the environment.[10] Colonization of solid electrodes to couple the microbial metabolism to the rest of the device is an essential part of the development of such systems. The metabolically critical members of a biofilm may be desired in high abundance. Electroactive biofilms can be exposed to large ranges of cell voltages possible from various soil microbiomes.[11] Furthermore, a single family within a microbial consortium may inordinately increase electroactivity.[10] Ancillary microbes may be incorporated into a biofilm, as one species may not be sufficient for maximal performance.[12] Therefore, microbe selection is essential to form useful biofilms. Selective microbial adhesion could also prevent colonization of pathogens or otherwise deleterious microbes through promotion of adhesion of benign species used as an inert layer.[13]

Received: March 6, 2020
Accepted: July 16, 2020
Published: July 16, 2020

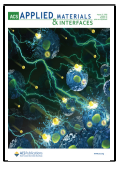

https://dx.doi.org/10.1021/acsami.0c04329
ACS Appl. Mater. Interfaces 2020, 12, 35767–35781

In addition to technological advances, manipulation of surface colonization can advance the fundamental study of microorganisms.[14] Inducing spaces between cells facilitates measurement of nanoscale features, which can be buried or hidden in clusters of cells. Intercellular interactions can be instigated by patterning different cell types next to one another. Figure 1 shows the features of colonization control through rational surface design—enrichment of desired cells on the surface or spatial patterning of cells into well-defined geometries.

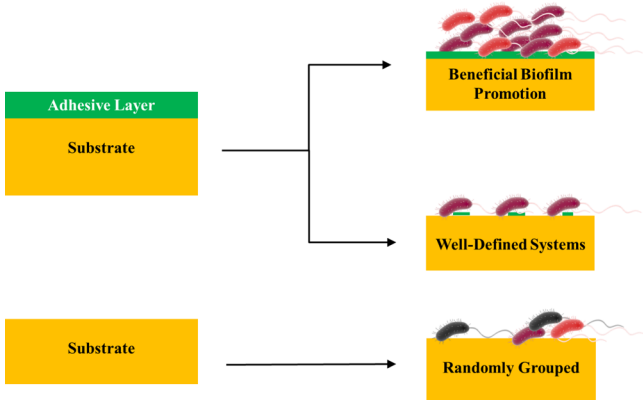

Figure 1. Control over microbe surface colonization. Higher densities of cells and cells of a strain of interest can be introduced on functionalized surfaces. Rather than unpredictable and erratic positioning of cells, well-defined systems can be created by promoting and reducing adhesion selectively.

The properties of a surface can determine whether or not a bacterium attaches and the composition of a bacterial colony that forms on the surface.[15,16] Physical properties of surfaces, such as positively charged surfaces, have been used to promote bacterial adhesion.[17−20] However, physical properties are susceptible to adulteration by the adsorption of a conditioning layer of the material. Specifically recognized chemical motifs may be less influenced by changing general properties of the overall surface. Saccharides are specifically recognized by microbes and have the advantages of water solubility, large stereochemical space, and abundant biosynthetic availability. Bacterial bonds to saccharides have the ability to become even more adherent to a surface under high shear force.[21] Accordingly, saccharides are known to be used by bacteria to mark surfaces for colonization.[22] The secretion of the exopolysaccharide (EPS) matrix is among the aspects of surface colonization affected by the internal signaling cascade in bacteria that is activated upon surface contact and detection.[2] Mannose and other saccharide monomers, such as galactose and glucose, are common motifs found in EPS molecules.[23]

Saccharide-binding proteins, known as lectins, may be presented by bacteria on the ends of hair-like appendages, known as pili. Several attachment pili, known as fimbriae, have been discovered that recognize surfaces and contribute to biofilm formation.[24] One well-studied fimbria is the type I pili that is composed mostly of FimA proteins and terminated with the FimH lectin.[25,26] This type I pilus binds the sugar mannose and is known to exist in *Escherichia coli* and several other gammaproteobacteria.[24,27,28] The attachment of bacteria that express FimH-terminated type I pili can be enhanced by engineering mannose-presenting surfaces. Whitesides and co-workers demonstrated the ability to attract *E. coli* to a surface covered with alkanethiols terminated with a mannose residue.[29]

The presence of multivalency can increase binding strength or rate more than the sum of an equivalent number of monovalent bonds.[30] The results of multivalent interactions between saccharides and their targets have been referred to as the cluster glycoside effect.[31] Between saccharides and isolated proteins, multivalency has been widely studied and thermodynamics and kinetics have been characterized.[32,33] On the scale of bacteria, it has been reported that increasing the density of mannose on a flat surface nonlinearly increases the number of *E. coli* cells that are adsorbed.[34,35]

Assembly on two-dimensional surfaces provides multiple binding sites of the saccharide of interest across the surface. However, these sites are limited in how densely they can be packed before steric crowding prevents further insertion of saccharides or occludes binding to the biological targets. To increase the valency of saccharides beyond the limit of a planar conformation, polymer scaffolding can be used. By extending the molecular layer further away from the surface, more of the three-dimensional space is occupied by saccharide units in a given surface area. The increased multivalency may then augment the interactions to saccharide binding partners. Such extension of mannose residues into three dimensions has been accomplished using branching oligosaccharides. Textor and co-workers reported that multivalent branched trimannose molecules adhered much more *E. coli* compared to monolayers of monovalent mannose-terminated molecules.[34] However, the size of the mannose cluster was optimal as a trimer and less *E. coli* attached to branched oligosaccharides with six or nine mannoses. The lower binding by the longer molecules may be due to the α-1,2 glycosidic bonding used on the outer mannose residues or because FimH is well fitted to trisaccharides, as has been described previously.[25] It has not yet been determined whether the increased adhesiveness of oligosaccharide mannose is due to increased valency, moiety density, or shape and receptor binding fit.

A glycopolymer can be constructed to present multiple monosaccharides rather than linking saccharide units in the manner of a polysaccharide, which is created by binding saccharide units directly to each other. This repeating monosaccharide polymer construction avoids the convolution between the alterations to the saccharide structure and the effects of multivalency. The availability of each of the saccharide unit's four hydroxyl groups is preserved, and the multivalent saccharide binding can be tested independently of effects due to modification of the saccharide structure. Surfaces functionalized with tethered polymers decorated with monosaccharide mannose pendants have been shown to enhance *E. coli* attachment while not enhancing attachment of *Staphylococcus aureus*.[36,37] These observations did not compare adhesion to mannose monomer layers that were not a part of polymeric protrusions.

Shewanella oneidensis is a model species of dissimilatory metal-reducing bacteria.[38] It contains the biochemical machinery to catalyze reactions between electron donors and a wide range of oxidants, and it is therefore desirable for bioelectrical systems.[39] *S. oneidensis* has been used to produce microbial fuel cells and biosynthetic sulfurous compounds.[40,41] Enriching key species, like *S. oneidensis*, in a microbial community can make useful genes functionally abundant and

https://dx.doi.org/10.1021/acsami.0c04329
ACS Appl. Mater. Interfaces 2020, 12, 35767−35781

Scheme 1. The structure of poly(mannose acrylate)thiol, referred to below as polymannose, is shown[a]

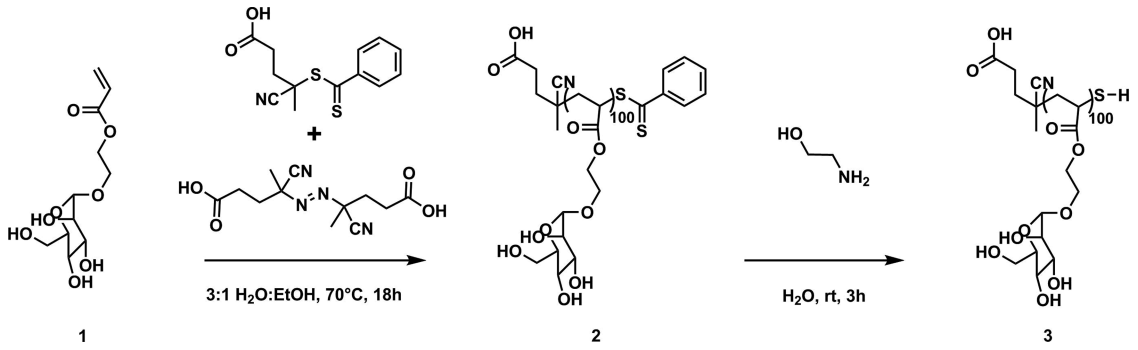

[a]The hydroxylethylacrylate center of the polymer has a general nonadhesiveness, while the monosaccharide pendants provide specific adhesiveness. The polymer is produced by reversible addition-fragmentation chain transfer, which provides a thiol upon aminolysis. Corresponding polymers with glucose, galactose, and *N*-acetylglucosamine were prepared by the same process with analogous starting monomers.

make beneficial biofilms more effective. Increased attachment of *Shewanella* has been achieved by air plasma pretreatment of carbon-based electrodes. The attachment concurrently increased current output of the associated fuel cell with a lower Coulombic efficiency.[42] *S. oneidensis* has also been engineered to express a gold-binding peptide on an outer membrane protein, LamB-5rGBP, which increased the attachment of the cells to the surface, but was associated with the loss of certain outer membrane proteins required for extracellular respiration.[43] DNA has been used to direct attachment of *S. oneidensis* as well.[44] Conductivity of complementary DNA strands appeared to facilitate electron transport between the cells and gold surfaces, and the current approximately quadrupled for cells linked to surfaces with DNA duplexes versus cells deposited without linkers. However, this method of DNA-facilitated attachment requires the cells to be chemically conjugated with complementary DNA through cleavage of bacterial saccharides with sodium periodate.

To promote adhesion specifically, mannosylated surfaces can be employed for *S. oneidensis* as it contains a mannose-binding lectin known as mannose-sensitive hemagglutinin (MSH).[45] Mannose-sensitive hemagglutinin is a type IV pilus that extends from the cell body and influences the motility and surface attachment of bacteria.[46] It has been described in a number of other gammaproteobacteria including *Vibrio cholerae*,[47,48] *Pseudoalteromonas tunicata*,[49] and *Aeromonas salmonicida*.[50] In *V. cholerae* El Tor, mannose-sensitive hemagglutinin has been shown to be used in forming biofilms on borosilicate surfaces.[48] Mannosylated surfaces can influence surface colonization, not only by providing a physical attachment point but also by modulating cellular colonization processes.

In this work, we approach the complex behavior of surface colonization by modifying a key component of surface interaction: the specific interaction between the MSH pili in *S. oneidensis* and mannose sugar motifs. The strength of this interaction may vary over time in response to an unknown number of variables. In *V. cholerae*, MSH pilus biogenesis can be affected by surface interactions as well as its internal signaling molecule cyclic-di-GMP, which means that pilus biogenesis can act as a function of multiple inputs.[51] Regardless of the other factors in MSH−mannose interaction, we found that it could be exploited by increasing the amount of accessible mannose. We successfully promoted surface adhesion of *S. oneidensis* and enriched the percentage of one strain over another. These findings are valuable for the rational design of beneficial biofilms.

RESULTS AND DISCUSSION

In this work, we synthesized glycopolymers decorated with various saccharides (Scheme 1) using a reversible addition-fragmentation chain transfer (RAFT) reaction. A related method has been reported previously where mannose units are attached to a polymer scaffold through the hydroxyl on the sixth carbon of mannose.[52] Here, we have attached each saccharide residue to the acrylate scaffold by the anomeric carbon. The glycosidic bond formed through the anomeric carbon not only stabilizes the α isomer of the saccharide but is also the configuration typically found in natural saccharide molecules. Nonreducing saccharides, which are bound through the anomeric carbon, tend to have increased biological activity compared to reducing saccharides.[53]

The polymeric structure is, as described above, intended to increase the number of saccharide binding sites along the surface normal as well as along the two dimensions parallel to the substrate surface. One saccharide residue was incorporated into the polymer chain per acrylate repeat unit to conserve the recognizability of the monosaccharide. Mannose, glucose, galactose, and *N*-acetylglucosamine saccharides were functionalized with an acrylate moiety and polymerized. For brevity, the poly(acrylate saccharide)s are referred to below by their saccharide type, e.g., polymannose. The polymerizable acrylate group of the glycopolymer monomer is linked to the saccharide unit by a hydroxyethyl group. The poly(hydroxyethyl acrylate) core structure that results in when the glycopolymers form is analogous to polymers that have reported low adhesiveness.[54,55]

Methods for producing polymers on a surface include physisorption, chemisorption of the formed polymer (known as "grafting to" the surface), and chemisorption of an initiator from which the polymer is formed in situ (known as "grafting from" the surface). The method used in this work is grafting to the surface, where the polymers are formed in solution and then bound to the surface through chemical bonding. The covalently bound chemisorption methods provide a stable bond to the surface that is not susceptible to changes in ion concentration and other factors of the medium.[56] The method grafting from a surface, although providing higher polymer density, may suffer from variable reaction completeness.[56,57] Polymer length is more homogeneous across the surface, and

https://dx.doi.org/10.1021/acsami.0c04329
ACS Appl. Mater. Interfaces 2020, 12, 35767−35781

Table 1. Glycopolymer Weight Average and Number Average Molecular Weight (M_w and M_n, Respectively), Dispersity ($Đ$), and Degree of Polymerization (DP_n)

saccharide	M_w [a]	M_n [a]	$Đ$ [a]	DP_n [a]	DP_n [b]
glucose	9600	6800	1.42	24	65
galactose	12000	8500	1.41	31	76
mannose	28700	16400	1.75	59	108
N-acetylglucosamine	14200	8400	1.68	27	76

[a]Aqueous gel permeation chromatography (GPC) relative to pullulan standards. [b]Comparison of the chain end and saccharide proton integrals with ^{1}H nuclear magnetic resonance (^{1}H NMR) spectroscopy.

surface-recombination side reactions are avoided when grafting to the surface rather than grafting from the surface.[58] The grafting to approach provides a known molecular structure and density of saccharides per polymer. Glycopolymers synthesized by RAFT featuring lactose and glucose have previously been grafted to surfaces to study *E. coli* adhesion.[59] Like other controlled polymerizations, RAFT offers better control over molecular weight and polydispersity than traditional chain polymerizations.[60]

Polymers synthesized by RAFT are conveniently terminated with a dithioester. The dithioester produces a free thiol upon aminolysis with ethanolamine, enabling facile self-assembly to gold surfaces. Gold is useful for electrodes in bioelectrical test systems because of its resistance to corrosion and high conductivity.[43] Electrodes of other metals and carbon are also used—compromising intrinsic conductivity for adhesiveness.[61−66] By functionalizing gold surfaces with a glycopolymer, we can introduce colony-promoting character to the conductive surface. The opposite end of the polymer from the sulfur group is terminated with a carboxylic acid group, which can be utilized for facile conjugation to amine-terminated surfaces or additional functionalization of the assembled poly(saccharide acrylate) layer.[67,68]

The degree of polymerization (DP_n), weight average and number average molecular weight (M_w and M_n, respectively), and dispersity ($Đ$) of the various glycopolymers used in these experiments are shown in Table 1. A linear relationship was observed between the DP_n of the polymers when measured by gel permeation chromatography (GPC) and when calculated from ^{1}H nuclear magnetic resonance (^{1}H NMR) spectroscopy. The degree of polymerization and molecular weight measurements by ^{1}H NMR spectroscopy were higher than those by GPC. This difference is likely due to the glycopolymer backbone and RAFT chain end being more hydrophobic than any component of pullulan and thus the glycopolymer having a smaller hydrodynamic volume than the polysaccharide of similar length. The glycopolymers would be expected to be more compact to minimize unfavorable interactions between their hydrophobic components and the aqueous solvent used in GPC.

Characterization of the glycopolymers after self-assembly on a surface was primarily achieved by X-ray photoelectron

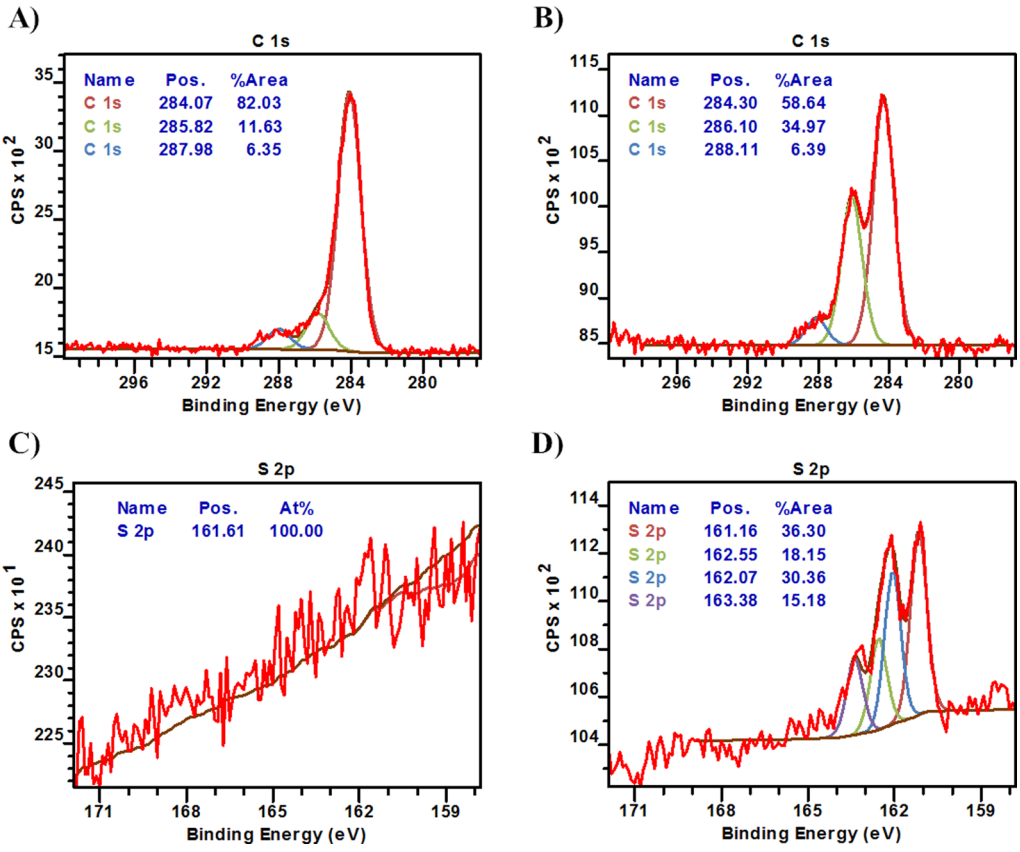

Figure 2. X-ray photoelectron spectra of glycopolymer surfaces. Bare gold (A) and polymannose on gold (B) carbon 1s spectra. C−C/C−H peaks of adventitious carbon and the deposited polymer are present at 284 eV in the bare gold and glycopolymer spectra. C−O bound carbon, present at 286 eV, and C=O bound carbon, present at 288 eV, increase in relative and total intensities as the glycopolymer is added to the surface. Bare gold (C) and polymannose (D) sulfur 2p spectra demonstrate the emergence of surface sulfur as the thiol-containing glycopolymer self-assembles.

https://dx.doi.org/10.1021/acsami.0c04329
ACS Appl. Mater. Interfaces 2020, 12, 35767−35781

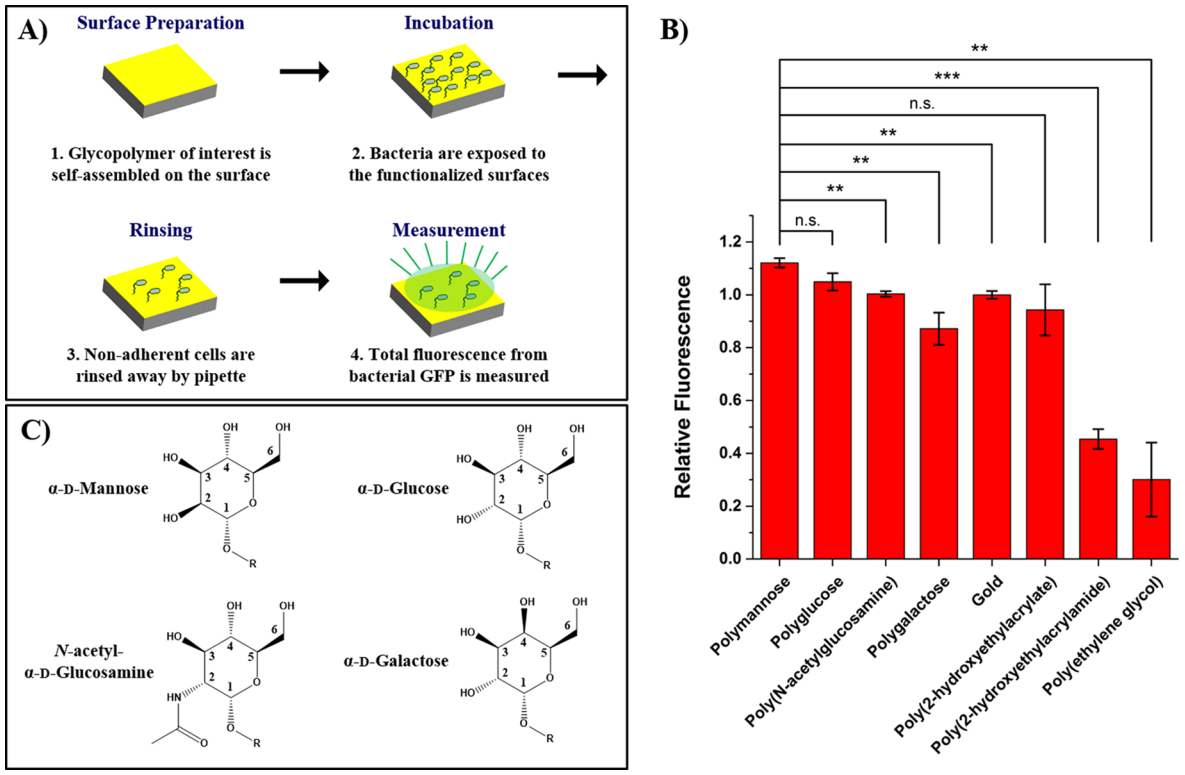

Figure 3. Adhesiveness of *S. oneidensis* cells to various surfaces as measured by total fluorescence. (A) Adhesiveness was measured by incubating fluorescent cells over polymer functionalized surfaces and rinsing away nonadherent cells. Fluorescence is plotted relative to the signal of cells adhered to bare gold. (B) Polymannose enables greater adhesion of *S. oneidensis*, which is diminished by changing the chirality of the second and fourth carbons of the poly(acrylate saccharide)s. Error bars indicate standard error of the mean (N = 4). (C) Saccharide motifs of the glycopolymers.

spectroscopy (XPS). The surfaces were measured after dissolving the glycopolymer in water with ethanolamine and exposing the solution to the gold surface for several days. Figure 2A shows the change in the line shape of the carbon 1s signal. Adventitious carbon, which adsorbs randomly on surfaces, is present in the spectrum of bare gold as a single peak at 284 eV.[69] The polymannose spectrum (Figure 2B) has three peaks corresponding to the C−C, C−O, and C=O sections of the polymer. The ratio of C−O to O−C−O and C=O is about 4:1, which corresponds roughly to the proportion of carbon species in the polymannose samples. Sulfur can be observed in the XPS spectra of the thiolated surfaces in the expected energy region at 162 eV (Figure 2D). The sulfur peak appears to be split into two doublets, with each doublet having an intensity ratio of 2:1 due to spin−orbit coupling. The two signals imply two metal sulfide binding modalities. Minimal oxidized sulfur is observed in the 166−171 eV window, even after weeks of storage in air. This result indicates good stability of the covalent bonding of the glycopolymers to the surface. No appreciable sulfur peak is observed on the bare gold substrate (Figure 2C). X-ray photoelectron spectra of the other glycopolymers show similar spectra to polymannose, as shown in Figures S7 and S8 in the Supporting Information. Ellipsometry, electrochemical desorption, water contact angle, tethered mannose monomer XPS spectra, and polarization modulation-infrared reflection-absorption spectra are also presented in the Supporting Information.

Adhesiveness of various polymers and saccharide moieties is shown in Figure 3. Monolayers of the glycopolymers were prepared and exposed to cultures of *S. oneidensis* that express green fluorescent protein (GFP). Nonadherent cells were rinsed away with phosphate-buffered saline (PBS), and the remaining cells were quantified by measuring the total fluorescence from the surface. Variances in GFP measurements as a result of cell proliferation were limited by exposing the cells to the surfaces while in nutrient poor solution, controlling the cell density and growth phase of cells applied to the surfaces, and measuring cells remaining on the surfaces immediately after rinsing away nonadherent cells. Polymannose shows the highest total fluorescence and is significantly brighter than the polygalactose and poly(*N*-acetylglucosamine) glycopolymers. The polymannose surfaces had 12.1 ± 2.3% by standard error of the mean (SEM) more fluorescence intensity than bare gold surfaces. Poly(hydroxyethylacrylate), which has the same core structures of the glycopolymers, showed similar fluorescence to bare gold surfaces. Poly(2-hydroxyethylacrylamide) and poly(ethylene glycol)-treated surfaces demonstrated lower fluorescence than all other samples.

The greater fluorescence indicates that polymannose promotes surface adhesion by *S. oneidensis* on this timescale of 18 h. Polyglucose has the most similar fluorescence to polymannose of the series of hexoses tested. Glucose differs from mannose by the stereochemistry of the hydroxyl on the second carbon, which faces toward the backbone of the polymer. Changing the chirality of only the second carbon hydroxyl is insufficient to significantly change bacterial recognition of the surface. Galactose, however, has inverted chirality at both the second and outward-facing fourth carbon with respect to mannose and binds significantly fewer bacteria.

https://dx.doi.org/10.1021/acsami.0c04329
ACS Appl. Mater. Interfaces 2020, 12, 35767−35781

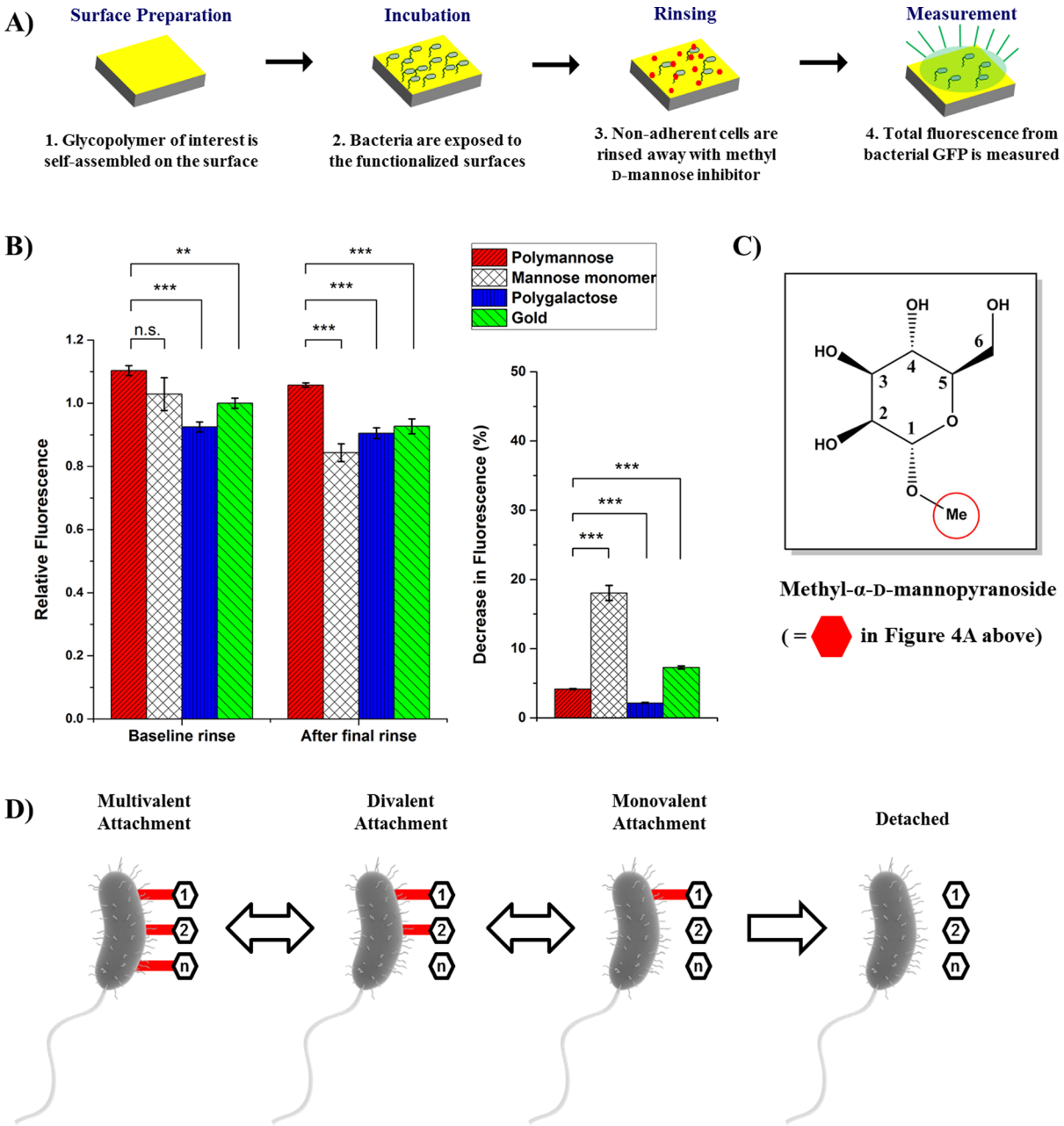

Figure 4. Persistence of cell adhesion after rinsing samples with methyl α-D-mannopyranoside, an analog of the surface-bound mannose units. (A) Method for testing robustness of cell adhesion using green fluorescent protein (GFP). (B) Both before and after mannoside inhibitor rinsing, more cells remained adhered to the polymannose surface than either polygalactose or bare gold. Tethered mannose monomer surfaces presenting a single mannoside residue per thiol head group originally adhered a similar amount of *S. oneidensis* to polymannose but lost more cells during methyl α-D-mannopyranoside rinsing. Error bars indicate standard error of the mean ($N = 5$). (C) Structure of the methyl α-D-mannopyranoside inhibitor. (D) Schematic of multivalent detachment.

The *N*-acetylglucosamine glycopolymer retains an intermediate number of bacteria between polyglucose and polygalactose. The stereochemistry of the saccharide residues appears to be more important than their size and functionality for *S. oneidensis* recognition of surface saccharides because the acetyl group appended to the second carbon substituent of poly(*N*-acetylglucosamine) is less impactful than the additional inversion of the fourth carbon chirality in polygalactose.

The greater influence of the fourth carbon hydroxyl over the second carbon hydroxyl we observed in *S. oneidensis* is consistent with the binding of *V. cholerae* cytolysin, which bonds to methyl α-D-mannose through the third and fourth carbon hydroxyls.[70] The related stereochemical importance may indicate that the *S. oneidensis* mannose-binding lectin (MshA) is homologous to *V. cholerae* lectins and forms β-prism domains.[70−72] The importance of fourth carbon hydroxyl also suggests that glycans with (1,4) glycosidic linkages are not as impactful for *S. oneidensis* colonization as saccharides that maintain a free hydroxyl on the fourth carbon.

Methyl α-D-mannopyranoside is a nonmetabolizable form of mannose, which can compete for binding of MSH lectin sites.[46] The methyl group is bound to the oxygen on the anomeric carbon of the mannose residue analogous to the core of the glycopolymers. Inhibition of binding between *E. coli* and

https://dx.doi.org/10.1021/acsami.0c04329
ACS Appl. Mater. Interfaces 2020, 12, 35767−35781

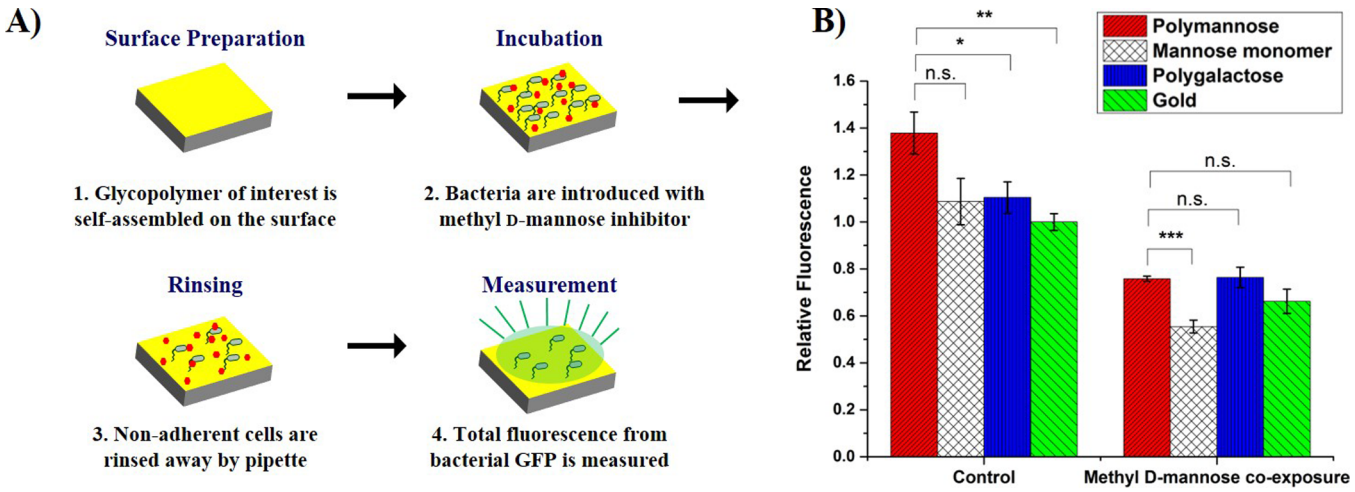

Figure 5. Inhibition of initial adhesion. (A) Simultaneous introduction of the inhibitor with cell culture. (B) With no methyl α-D-mannopyranoside, results are as observed with other measurements and polymannose samples have the greatest fluorescence. Mixing methyl α-D-mannopyranoside with the original cell culture, before exposure to the substrate surfaces, removes the difference between polymannose, polygalactose, and bare gold in adhered cells. All samples, particularly the tethered mannose monomer, adhere less *S. oneidensis* when incubated with methyl α-D-mannopyranoside. Error bars indicate standard error of the mean (N = 4).

copolymers featuring a poly(mannose methacrylate) arm by methyl α-D-mannopyranoside has been demonstrated previously.[73] The methyl α-D-mannopyranoside inhibitor dissolved in PBS was used to rinse bacteria from the various surfaces to test the strength of attachment. During these rinses, the culture medium was removed and replaced with solution without cells, which greatly diminishes the attachment rate of the bacteria. The detachment rate thus becomes the governing factor in the net attachment rate.

Rinsing the bacteria laden surfaces with methyl α-D-mannopyranoside solution caused a decrease in the total GFP fluorescence, suggesting that fewer cells were adhered (Figure 4). The decrease in total fluorescence caused by rinsing with methyl α-D-mannopyranoside solution was disproportionately larger for the tethered mannose monomer (11-[(*p*-phenyl-α-D-mannopyranosyl)amino-carbonylmethoxyhexa(ethoxy)]undec-1-yl-thiol) surfaces, which have a single mannoside residue per molecule assembled on the surface. Tethered mannose monomers became statistically distinguishable from polymannose after rinsing. Both glycopolymer samples tested retained more of the initially adhered cells than bare gold surfaces. The percentage decreases in total fluorescence from before rinsing with methyl α-D-mannopyranoside were as follows: 4.2 ± 1.6% (SEM) for polymannose surfaces, 18.1 ± 5.8% (SEM) for the tethered mannose monomer, 2.2 ± 2.5% (SEM) for polygalactose, and 7.3 ± 2.9% (SEM) for bare gold. The decrease in fluorescence indicates faster detachment of cells adhered to tethered mannose monomer surfaces than the glycopolymer surfaces.

The three-dimensional multivalency of the glycopolymers seems to be responsible for slowing the detachment rate of adherent cells considering that the monovalent mannose-terminated monolayers were more easily removed. With multivalent attachment, the rupture of one bond does not fully detach the binding partners and time is allowed for rebinding to occur. On the scale of the bacteria, this means that the detachment of one saccharide-lectin pair does not fully release a cell from the surface (Figure 4D). Other saccharides and bacterial recognition sites remain localized, and reattachment of the unbound lectin can occur more rapidly. By having multiple binding sites, a cell is therefore kinetically hindered from releasing from the surface. In addition to the mannose bonds directly holding a bacterium in place, the multivalent effect may act indirectly through surface sensing. As more sensory receptors are bound to target molecules, integration of their signal over time would be larger. Multivalent attachment of surface sensory receptors could then increase the colonization response and more rapidly establish strong attachment of the cell to the surface through secondary binding sites.

When methyl α-D-mannopyranoside was added to the bacterial culture before exposure to a surface, less adhesion was observed (−0.62 ± 0.09 (SEM) for polymannose, −0.53 ± 0.10 (SEM) for tethered mannose monomers, −0.34 ± 0.08 (SEM) for polygalactose, and −0.34 ± 0.06 (SEM) for bare gold surfaces, all in arbitrary units of relative fluorescence), and the difference between adhesiveness of glycopolymers surfaces and bare gold was no longer significant (Figure 5). Tethered mannose monomer surfaces showed the lowest fluorescence of all surface types when *S. oneidensis* is incubated with methyl α-D-mannopyranoside.

Rinsing with the mannose inhibitor after cells have attached to the surfaces, as presented in Figure 4, shows the robustness of *S. oneidensis* colonization on polymannose, once established. Concurrent exposure of the methyl α-D-mannopyranoside and the cell culture to the surface (Figure 5) probes the importance of steady-state mannose binding and sensing and provides some mechanistic insights. The resistance to methyl α-D-mannopyranoside-induced detachment observed in Figure 4 appears to be kinetic in nature because the enhanced persistence of adhered cells on polymannose is removed when the system is provided time to equilibrate as in Figure 5. Transiently introducing methyl α-D-mannopyranoside with rinsing produces a more dynamic system than concurrent exposure lasting the entire incubation period. Both cell−surface association rates and dissociation rates of the systems presented in Figure 5 are influenced by methyl α-D-mannopyranoside, whereas in Figure 4, the inhibitor largely affects the dissociation rate as cells are already attached when methyl α-D-mannopyranoside is introduced and planktonic

https://dx.doi.org/10.1021/acsami.0c04329
ACS Appl. Mater. Interfaces 2020, 12, 35767−35781

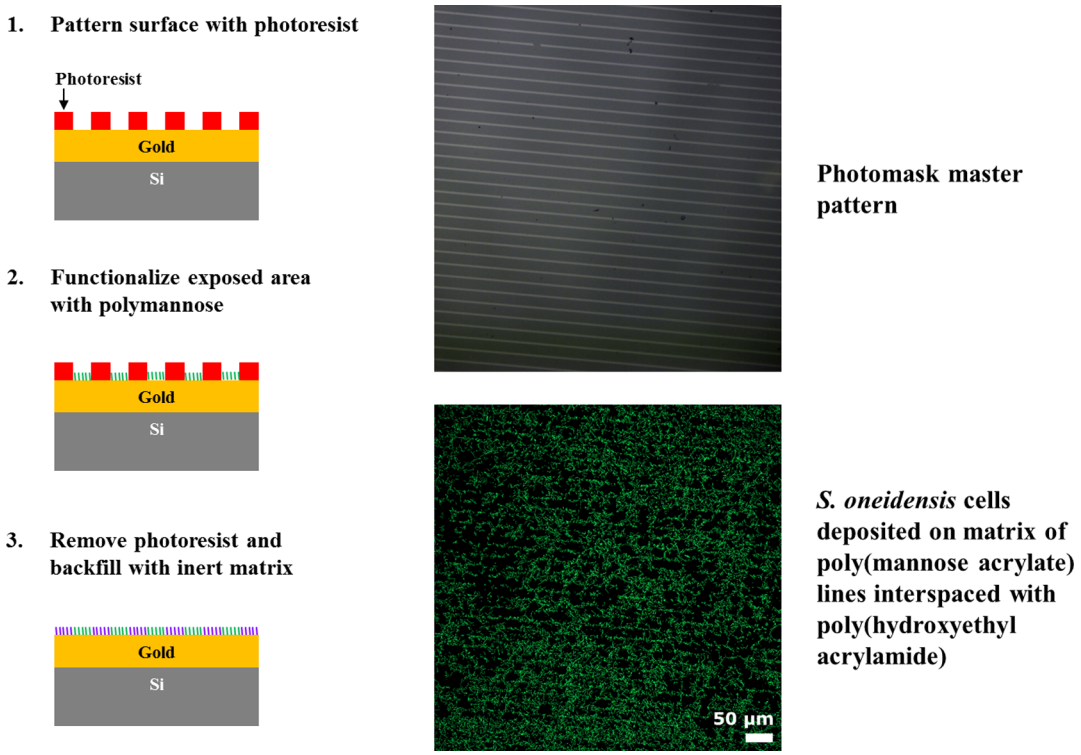

Figure 6. Demonstration of the ability to control *S. oneidensis* adhesion to a surface was performed with a molecular pattern of polymannose in a poly(2-hydroxyethylacrylamide) matrix. The polymannose was deposited in 2 μm lines interspersed with poly(2-hydroxyethylacrylamide) with a periodicity of 10 μm. The attraction of the polymannose retains cells over the area where it is deposited.

cells are removed. Our results suggest that previously reported kinetic descriptions of multivalency in cluster glycosides also concern systems on the scale of microbial cells.[30,33,74]

Mechanistically, the ability of methyl α-D-mannopyranoside to inhibit the enhanced cellular attachment on polymannose surfaces implies the structures of the mannoside units as the causative agents that enhance attachment. The free methyl α-D-mannopyranoside can occlude recognition sites on the bacteria; once the receptors are blocked, mannose-dependent adhesiveness is presumably diminished. Furthermore, it appears that the attachment enhancement is the result of a direct physical linkage between the bacteria and the surface, rather than the result of signaling cascades responding to sensing of mannoside units, because the addition of dissolved mannoside units decreased attachment and the addition of surface-tethered mannoside units increased attachment.

Tethered mannose monomer surfaces appear less adhesive to *S. oneidensis* than polymannose or polygalactose with methyl α-D-mannopyranoside present. One explanation for this result is that tethered mannose monomer surfaces have lower mannose-lectin-independent—thus, nonspecific—adhesiveness than the glycopolymers. The ethylene glycol linkage in the tether that attaches the mannose monomer to the gold surface could reduce surface adhesiveness. Nonspecific multivalency between the glycopolymers and non-MSH binding sites could also contribute to the differences between tethered mannose monomers and the glycopolymers. The glycopolymer saccharide pendants could undergo reattachment if multiple pendants are physisorbed to a particle. In other words, nonspecific binding sites that are not lectins can allow reattachment of a severed bond as long as other bacterium–surface bonds keep the saccharides pendants localized to either the previous binding location or a new one. If the galactose units of the polygalactose surfaces are binding to *S. oneidensis* nonspecifically, these interactions could also explain the resistance to methyl α-D-mannopyranoside rinses seen in polygalactose (Figure 4), which has a similar relative magnitude to polymannose surfaces. If only nonspecific interactions were involved, the adhesiveness of the mannose and galactose units to nonspecific bonding partners is expected to be very similar as only the stereochemistry differs in the molecules. Dipole interactions and hydrogen bonding have similar opportunities for physical attachment in either type of saccharide pendant. The glycopolymers would then have similar levels of attached cells when the mannose-binding sites are filled by methyl α-D-mannopyranoside.

Another possibility for why tethered mannose monomers are more affected by the addition of methyl α-D-mannopyranoside is that polymannose may be able to interact with a partially filled array of lectins more effectively due to its expanded valency. Mannose-dependent attachment mechanisms may be present in reduced form if the system is subsaturated. Polygalactose may interact with other lectins produced by *S. oneidensis* and retain adhesiveness relative to tethered mannose monomers. Galactose-dependent binding could also explain the resistance to methyl α-D-mannopyranoside rinses in Figure 4. The differences between adhesiveness due to partial availability of mannose lectins binding to polymannose surfaces and galactose lectins binding to polygalactose surfaces is not distinguishable if this is the case.

The inhibition of *S. oneidensis* adhesion with a soluble mannoside suggests the activity of mannose sensitive hemagglutinin (MSH). The ratio of wild type *S. oneidensis* to Δ*mshA-D* adhered to various surfaces after coculture deposition is shown in Figure S1. The enrichment of wild

https://dx.doi.org/10.1021/acsami.0c04329
ACS Appl. Mater. Interfaces 2020, 12, 35767−35781

type on polymannose surfaces indicates the influence of MSH on the attachment mechanism.

S. oneidensis was stimulated into a series of lines by molecularly patterning a gold surface with polymannose by conventional photolithography (Figure 6). Polymannose was self-assembled around a photoresist layer. The photoresist was removed, and the gaps between the polymannose regions were backfilled with poly(2-hydroxyethylacrylamide). The increased adhesion of polymannose enables spatial control over bacterial surface colonization. With control over colonization, arbitrary patterns can be used for the fundamental study of cell interaction with each other, coculture interaction with successive deposition of various strains or species, or other spatially important properties such as bacterial appendages, which can be unidentifiable in a monolayer of cells.

PROSPECTS

In this work, we employed glycopolymers presenting a monosaccharide on each of their side chains. These saccharides conserve hydroxyl groups by binding only with the anomeric carbon and thus preserve known monosaccharide recognition by bacteria. Further work could incorporate oligosaccharide units branching off of the polymeric support. Such oligosaccharides can be homooligosaccharide units utilizing the same saccharides or heterooligosaccharides using combinations of different saccharide types. As the trisaccharide motif has been found to increase *E. coli* binding significantly, other oligosaccharide configurations may offer substantial avidity and specificity for targeted microbes.[25] Psl is a polysaccharide used in bacterial surface sensing that may be worth emulating.[22] By multiplexing the design space of saccharide presenting surfaces, we expect high specificity for chosen microbial targets.

Microbial bioelectrical systems require interfaces that exchange electrons with microbes. For such applications, the improved adhesive qualities of the glycopolymer layer are balanced against the electrical conductivity of the material. Mannose-decorated polymers with a conductive backbone, such as polyaniline or poly(3,4-ethylenedioxythiophene) polystyrene sulfonate (PEDOT:PSS), could be synthesized to optimize both conductivity and adhesiveness of the biofilm−electrode interface. The tradeoff in interfacial electrical conductivity versus increased attachment and cellular meshing with the surfaces of different types of polymer layers could then be investigated, first measuring the impedance of various types of glycopolymer films, then testing the impact of adulterants in the culture supernatant on the surface's conductivity over time, and finally measuring the current output over time from microbial fuel cells with various types of mannosylated anodes. The electrical conductivities of these polymer films may also be increased by allowing electron transport between the molecules coating the surface. Engineering the polymer layer to have sub-monolayer coverage and exposing conductive patches of the substrate are ways to encourage cellular interactions without obscuring electron transport.

The time dependence of bacterial attachment and growth dynamics should also be investigated. The kinetic nature of the resistance to methyl α-D-mannopyranoside inhibition by the glycopolymers studied here emphasizes the importance of cellular attachment and detachment rates. Studying the strength of equilibrium binding alone misses the dynamic features of microbial surface colonization. Real-time measurements are necessary to compare the dynamics of various surface types being colonized. Moreover, studies that measure only initial and final time points have their conclusions limited by the convolution of cellular growth, death, attachment, and detachment. By separating the rates of each of these processes, mechanistic principles are derivable.

The cellular pattern demonstrates the directing capability of the polymer layer and can be used as a tool for further experimentation. The fidelity of the bacterial pattern on the molecular pattern may be further improved by investigating rinsing techniques. As rinsing is the mechanism used to remove cells in the undesired areas, it is an important parameter to understand. Improvements to bacterial patterning are also expected if the adhesiveness of the glycopolymer is improved, as suggested above. Providing a more nutritious application medium and time for the attached cells to divide may increase the cell packing density on the desired areas.

When one cell type is spatially patterned and another cell type is placed next to it, interactions between cells, such as intercellular communication, can be observed. Measurement of nanoscale features, especially with surface-sensitive techniques, is facilitated with reproducible, well-defined colonization; nanoscopic features in microbial communities can be buried or hidden in clusters of cells. The cellular interactions with boundaries of surface types can also be observed on the chemically patterned surface.

Colonization enhancement of WT *S. oneidensis* and enrichment against the Δ*mshA-D* knockout strain (Figure S1) suggest the possibility of designing a system to enrich *S. oneidensis* versus any other microbe that does not express mannose recognition. Enrichment enhances utilization of strains in mixed populations of microbes, where a desired strain might be excluded or have reduced presence against faster surface colonizers. If a polymannose surface can enrich *S. oneidensis* against other endemic microbes in its native environment, a more electroactive biofilm may be produced by amplifying the proportion of the key species. The scope of the ability to enrich a desired strain, species, or functionally active population from other types of cells should be explored. To examine the ability of the glycopolymer surfaces to select a species of interest, *S. oneidensis* colonization should be tested against a fast biofilm-forming species that binds to surfaces by a method that does not use mannose. Selection of a deletable gene with glycopolymers could be expanded with synthetic genetic sequences that express a saccharide receptor alongside useful genes, thus amplifying genes of interest in an area with the corresponding saccharide. The *mshA* gene could act as a reporter if another gene of interest was expressed proximally on the genome or on a plasmid. In general, controlling colonization enables modulation of a consortium of microbes to create designer microbiomes for uses such as biosynthesis or medical treatment.

Many biotechnologies and further studies may be designed using saccharides to colonize surfaces selectively with microbial strains of choice. Beyond promoting functional or useful genes in the genome of a biofilm, promoting benign microbes could prevent pathogens or otherwise deleterious microbes from attaching to a surface. The process of benign fouling of a surface could be a useful general strategy addressable by glycopolymer functionalization.

CONCLUSIONS

We synthesized glycopolymers presenting branching monosaccharide units and assembled them onto gold surfaces to

https://dx.doi.org/10.1021/acsami.0c04329
ACS Appl. Mater. Interfaces 2020, 12, 35767−35781

influence the surface colonization by the bacteria *S. oneidensis*. The poly(mannose acrylate) glycopolymer promoted adhesion of 12.1 ± 2.3% (SEM) more cells versus bare gold surfaces. When the wild-type strain was codeposited with a Δ*mshA-D* knockout strain, the fraction of cells that contained the *mshA-D* genes was increased by 5.4 ± 2.4% (SEM). This enhancement indicates the strain selectivity of the surface and the importance of mannose-sensitive hemagglutinin pili's MshA lectin.

The persistence of the cellular attachment was investigated by rinsing the adhered cells with methyl α-D-mannopyranoside, an inhibitor for binding to the MSH attachment pili. Following the rinses with methyl α-D-mannopyranoside, the glycopolymer samples presented the smallest decrease of attached cells suggesting stable colonization (the decreases in total fluorescence were 4.2 ± 1.6% (SEM) for polymannose surfaces and 2.2 ± 2.5% (SEM) for polygalactose surfaces versus 18.1 ± 5.8% (SEM) for tethered mannose monomers and 7.3 ± 2.9% (SEM) for bare gold surfaces). By adding the inhibitor before surface exposure, the specific adhesiveness of polymannose is removed relative to polygalactose and bare gold surfaces. This result indicates that mannose-specific binding is the driving factor for the augmented *S. oneidensis* attachment to polymannose surfaces. The retention of cells adhering to polymannose in the presence of methyl α-D-mannopyranoside appears to be a kinetic effect as the inhibitor must be concurrently incubated for several hours to equalize the samples. The three-dimensional multivalency of glycopolymer samples appears to be responsible for the enhanced adhesiveness because tethered mannose monomer surfaces do not retain as many cells upon inhibition of surface binding. The ability to pattern *S. oneidensis* on polymannose surfaces was also demonstrated in this work.

Using the glycopolymer surfaces, we have driven bacterial colonization, enriched one strain of the bacteria against another, and induced where bacteria attach. These capabilities enable new experimental design and technological innovation. Rational design of bioelectrical technologies is reliant on surface-colonizing microbes. Our model system targets bioelectrical systems by using the metal-reducing *S. oneidensis* as the microbe and conductive, nonoxide forming gold as the solid surface. Generally, our findings that a poly(monosaccharide acrylate)-functionalized surface can produce stable initial attachment and that saccharide-lectin pairs are promising for biofilm customization can be applied to other types of beneficial or benign microbes.

MATERIALS AND METHODS

Saccharide Acrylate Monomer Syntheses. *2-O-(α-D-Mannosyl)hydroxyethyl Acrylate.* 1,2,3,4,6-Pentaacetyl-α,β-D-mannose: Acetic anhydride (50 mL, 0.53 mol) was added to a solution of D-mannose (10 g, 55 mmol) dissolved in pyridine (100 mL) and stirred for 24 h. The solution was concentrated in vacuo and added to cold deionized (DI) water. The product was taken up in dichloromethane (DCM) and washed with a saturated sodium bicarbonate solution (2×), washed with brine, dried with sodium sulfate, and concentrated in vacuo (12.7 g, 59%). ^{1}H NMR (300 MHz, $CDCl_3$): δ 6.10 (d, H-1α), 5.89 (d, H-1β), 5.10−5.50 (m, H-2,3,4), 3.71−4.30 (m, H-5α, H2-6), 3.83 (m, H-5β), 2.00−2.19 (s, 15H, 5 CH_3).

2-*O*-(2,3,4,6-Tetraacetyl-α-D-mannosyl)hydroxyethyl acrylate: Boron trifluoride etherate (2.7 mL, 21 mmol) was added dropwise to a stirring solution of 1,2,3,4,6-pentaacetyl-α,β-D-mannose (2.7 g, 6.9 mmol) and hydroxyethyl acrylate (1.0 mL, 8.7 mmol) dissolved in DCM (25 mL) cooled in an ice bath. The solution was allowed to warm to room temperature after the addition was completed and stirred for 96 h. The reaction was washed with DI water (3×), a saturated solution of sodium bicarbonate, and brine. The organic solution was dried with sodium sulfate, concentrated, and isolated by silica column chromatography using 11:9 ethyl acetate in hexanes as an eluent (1.5 g, 49%). ^{1}H NMR (300 MHz, $CDCl_3$): δ 6.43 (d, 1H, CH_2=CH), 6.15 (m, CH_2=CH), 5.87 (d, 1H, CH_2=CH), 5.20−5.40 (m, H-2,3,4), 4.87 (d, H-1), 4.34 (m, 2H, OCH_2CH_2OC=O), 4.03−4.27 (m, 3H, H-5, H2-6), 3.78−3.90 (m, 2H, OCH_2CH_2OC=O), 1.99−2.17 (s, 12H, 4 CH_3).

2-*O*-(α-D-Mannosyl)hydroxyethyl acrylate: Sodium methoxide (1 mL, 0.2 M) was added to a solution of 2-*O*-(2,3,4,6-tetraacetyl-α-D-mannosyl)hydroxyethyl acrylate (1.5 g, 3.4 mmol) dissolved in DCM (5 mL) and methanol (4 mL) and stirred for 3 min before quenching with DOWEX 50WX8 ion-exchange resin for 30 min. The glycomonomer was isolated by silica column chromatography using 2:8 methanol in DCM as an eluent (368 mg, 39%). ^{1}H NMR (300 MHz, MeOD): δ 6.40 (d, 1H, CH_2=CH), 6.19 (m, CH_2=CH), 5.90 (d, 1H, CH_2=CH), 4.80 (d, H-1), 4.34 (m, 2H, OCH_2CH_2OC=O), 3.94 (m, 1H, OCH_2CH_2OC=O), 3.58−3.81 (m, 7H, H-2,3,4,5, H2-6, OCH_2CH_2OC=O).

2-O-(β-D-Glucosyl)hydroxyethyl Acrylate. 1,2,3,4,6-Pentaacetyl-β-D-glucose: D-Glucose (6 g, 33 mmol) was added gradually to a solution of sodium acetate trihydrate (3 g, 22 mmol) dissolved in acetic anhydride (42 mL, 0.45 mol) previously heated at 140 °C for 20 min. The reaction was removed from heat after 15 min and allowed to cool to room temperature before gradually pouring into ice water and allowed to precipitate at 4 °C overnight. The solid was collected by vacuum filtration and recrystallized in ethanol (6.9 g, 53%). ^{1}H NMR (300 MHz, $CDCl_3$): δ 5.73 (d, H-1), 5.10−5.30 (m, H-2,3,4), 4.10−4.30 (m, 2H, H2-6), 3.85 (m, H-5), 2.01−2.11 (s, 15H, 5 CH_3).

2-*O*-(2,3,4,6-Tetraacetyl-β-D-glucosyl)hydroxyethyl acrylate: Boron trifluoride etherate (2.7 mL, 21 mmol) was added dropwise to a stirring solution of 1,2,3,4,6-pentaacetyl-β-D-glucose (2.7 g, 7 mmol) and hydroxyethyl acrylate (1.2 mL, 10.4 mmol) dissolved in DCM (25 mL) cooled in an ice bath. The solution was allowed to warm to room temperature after the addition was completed and stirred for 16 h. The reaction was washed with DI water (2×), a saturated solution of sodium bicarbonate (2×), and brine. The organic solution was dried with sodium sulfate, concentrated, and isolated by silica column chromatography using 1:1 ethyl acetate in hexanes as an eluent (1.7 g, 55%). ^{1}H NMR (300 MHz, $CDCl_3$): δ 6.42 (d, 1H, CH_2=CH), 6.11 (m, CH_2=CH), 5.85 (d, 1H, CH_2=CH), 5.00−5.20 (m, H-2,3,4), 4.55 (d, H-1), 4.10−4.30 (m, 4H, H2-6, OCH_2CH_2OC=O), 4.01 (m, 1H, OCH_2CH_2OC=O), 3.80 (m, 1H, OCH_2CH_2OC=O), 3.70 (m, H-5), 2.00−2.10 (s, 12H, 4 CH_3).

2-*O*-(β-D-Glucosyl)hydroxyethyl acrylate: Sodium methoxide (2 mL, 0.2 M) was added to a solution of 2-*O*-(2,3,4,6-tetraacetyl-β-D-glucosyl)hydroxyethyl acrylate (1.7 g, 4 mmol) dissolved in DCM (8 mL) and methanol (10 mL) and stirred for 7 min before quenching with DOWEX 50WX8 ion-exchange resin for 30 min. The glycomonomer was isolated by silica column chromatography using 2:8 methanol in DCM as an eluent (207 mg, 20%). ^{1}H NMR (300 MHz, MeOD): δ 6.42 (d, 1H, CH_2=CH), 6.19 (m, CH_2=CH), 5.91 (d, 1H, CH_2=CH), 4.35 (m, 3H, H-1, OCH_2CH_2OC=O), 4.12 (m, 1H, OCH_2CH_2OC=O), 3.88 (m, 2H, H2−6, OCH_2CH_2OC=O), 3.69 (dd, 1H, H2-6), 3.31 (m, H-3,4,5), 3.19 (t, H-2).

N-Acetylglucosamine Acrylate Monomer. 2-Acetamido-1,3,4,6-tetraacetyl-2-deoxy-α-D-glucose: Acetic anhydride (47 mL, 0.5 mol) was added to a solution of D-glucosamine hydrochloride (10 g, 46 mmol) and 4-dimethylaminopyridine (10 mg) dissolved in pyridine (50 mL) and stirred for 72 h. The reaction was chilled in an ice bath, and sodium bicarbonate was gradually added until no gas evolved. The product was extracted with ethyl acetate, washed with brine, concentrated in vacuo, and crystallized with ethanol (15 g, 84%). ^{1}H NMR (300 MHz, $CDCl_3$): δ 6.18 (d, H-1), 5.61 (d, H-4),

https://dx.doi.org/10.1021/acsami.0c04329
ACS Appl. Mater. Interfaces 2020, 12, 35767−35781

5.24 (m, H-2,3), 4.52 (m, −NH), 4.27 (dd, 1H, H2-6), 4.09 (dd, 1H, H2-6), 4.02 (m, H-5), 1.95−2.21 (s, 15H, 5 CH_3).

2-Methyl-2-(3,4,6-triacetyl-1,2-dideoxy-α-D-glucosyl)-[2,1-*d*]-2-oxazoline: Trimethylsilyl trifluoromethanesulfonate (1 mL, 5.5 mmol) was added to a solution of 2-acetamido-1,3,4,6-tetraacetyl-2-deoxy-α-D-glucose (2.0 g, 5.1 mmol) dissolved in dichloroethane (9 mL) and heated at 50 °C for 21 h before quenching with triethylamine (1 mL). The reaction was washed with DI water (4×) and dried with sodium sulfate. The product was isolated by silica column chromatography using 9:1 ethyl acetate in hexanes as an eluent (1.5 g, 88%). ^{1}H NMR (300 MHz, $CDCl_3$): δ 5.94 (d, H-1), 5.24 (t, H-3), 4.91 (d, H-4), 4.16 (m, H-5, H2-6), 3.60 (m, H-2), 2.07 (s, 12H, 4 CH_3).

2-*O*-(2-Acetamido-3,4,6-triacetyl-2-deoxy-β-D-glucosyl)-hydroxyethyl acrylate: Trifluoromethanesulfonic acid (25 μL, 0.3 mmol) was added to a solution of 2-methyl-2-(3,4,6-triacetyl-1,2-dideoxy-α-D-glucosyl)-[2,1-*d*]-2-oxazoline (1.0 g, 3 mmol) and hydroxyethyl acrylate (0.54 mL, 4.7 mmol) dissolved in dichloroethane (8.3 mL) and heated at 60 °C for 6 h before quenching with triethylamine and diluting with DCM. The reaction was washed with DI water (2×), washed with brine, dried with sodium sulfate, and crystallized from diethyl ether (1.0 g, 75%). ^{1}H NMR (300 MHz, $CDCl_3$): δ 6.44 (d, 1H, CH_2═CH), 6.14 (m, CH_2═CH), 5.87 (d, 1H, CH_2═CH), 5.67 (d, H-4), 5.30 (t, H-2), 5.04 (t, H-3), 4.78 (d, H-1), 4.43 (m, −NH), 4.25 (m, 2H, OCH_2CH_2OC═O), 4.15 (dd, 1H, H2-6), 4.02 (m, 1H, OCH_2CH_2OC═O), 3.86 (m, 2H, H2-6, OCH_2CH_2OC═O), 1.91−2.08 (s, 12H, 4 CH_3).

2-*O*-(2-Acetamido-2-deoxy-β-D-glucosyl)hydroxyethyl acrylate: Sodium methoxide (1 mL, 0.2 M) was added to a solution of 2-*O*-(2-acetamido-3,4,6-triacetyl-2-deoxy-β-D-glucosyl)hydroxyethyl acrylate (511 mg g, 1.1 mmol) dissolved in DCM (2.5 mL) and methanol (1.5 mL) and stirred for 1 min before quenching with DOWEX 50WX8 ion-exchange resin for 30 min. The glycomonomer was isolated by silica column chromatography using 2:8 methanol in DCM as an eluent (106 mg, 29%). ^{1}H NMR (300 MHz, MeOD): δ 6.40 (d, 1H, CH_2═CH), 6.16 (m, CH_2═CH), 5.88 (d, 1H, CH_2═CH), 4.47 (d, H-1), 4.28 (m, 2H, OCH_2CH_2OC═O), 4.04 (m, 1H, OCH_2CH_2OC═O), 3.88(dd, 1H, H2-6), 3.78 (m, 1H, OCH_2CH_2OC═O), 3.65 (m, 3H, H-3,4, H2-6), 3.46 (t, H-2), 3.32 (m, H-5).

2-O-(β-D-Galactosyl)hydroxyethyl Acrylate. 1,2,3,4,6-Pentaacetyl-β-D-galactose: D-Galactose (20 g, 111 mmol) was added gradually to a solution of sodium acetate trihydrate (10 g, 74.5 mmol) dissolved in acetic anhydride (200 mL, 2.1 mol) previously heated at 120 °C for 30 min. The reaction was removed from heat after an hour and allowed to cool to room temperature before gradually pouring into a solution of sodium bicarbonate. Additional sodium bicarbonate was added until no gas was produced upon addition. The solid was taken up in DCM and washed with saturated sodium bicarbonate (4×), DI water, and brine. The organic solution was dried with sodium sulfate, concentrated, and covered with diethyl ether at −20 °C. The white crystals were collected by vacuum filtration (24.84 g, 67%). ^{1}H NMR (300 MHz, $CDCl_3$): δ 5.71 (d, H-1), 5.43 (d, H-4), 5.34 (dd, H-2), 5.09 (dd, H-3), 4.15 (m, 2H, H2-6), 4.05 (t, H-5), 2.00−2.17 (s, 15H, 5 CH_3).

2-*O*-(2,3,4,6-Tetraacetyl-β-D-galactosyl)hydroxyethyl acrylate: Boron trifluoride etherate (2.0 mL, 16 mmol) was added dropwise to a stirring solution of 1,2,3,4,6-pentaacetyl-β-D-galactose (2.0 g, 5.1 mmol) and hydroxyethyl acrylate (1.2 mL, 10.4 mmol) dissolved in DCM (25 mL) cooled in an ice bath. The solution was allowed to warm to room temperature after the addition was completed and stirred for 16 h. The reaction was washed with DI water (3×), a saturated solution of sodium bicarbonate, and brine. The organic solution was dried with sodium sulfate, concentrated, and isolated by silica column chromatography using 7:3 ethyl acetate in hexanes as an eluent (2.0 g, 87%). ^{1}H NMR (300 MHz, $CDCl_3$): δ 6.44 (d, 1H, CH_2═CH), 6.13 (m, CH_2═CH), 5.87 (d, 1H, CH_2═CH), 5.39 (d, H-4), 5.21 (dd, H-2), 5.03 (dd, H-3), 4.54 (d, H-1), 4.32 (m, 2H, OCH_2CH_2OC═O), 4.15 (m, 3H, H2-6, OCH_2CH_2OC═O), 3.93 (t, H-5), 3.83 (m, 1H, OCH_2CH_2OC═O), 1.99−2.16 (s, 12H, 4 CH_3).

2-*O*-(β-D-Galactosyl)hydroxyethyl acrylate: Sodium methoxide (300 μL, 0.2 M) was added to a solution of 2-*O*-(2,3,4,6-tetraacetyl-β-D-galactosyl)hydroxyethyl acrylate (2.0 g, 4.5 mmol) dissolved in methanol (20 mL) and stirred for 10 min before quenching with DOWEX 50WX8 ion-exchange resin for 30 min. The glycomonomer was isolated by silica column chromatography using 2:8 methanol in DCM as an eluent (357 mg, 29%). ^{1}H NMR (300 MHz, MeOD): δ 6.39 (d, 1H, CH_2═CH), 6.17 (m, CH_2═CH), 5.87 (d, 1H, CH_2═CH), 4.33 (m, 2H, OCH_2CH_2OC═O), 4.26 (d, H-1), 4.09 (m, 1H, OCH_2CH_2OC═O), 3.60−3.80 (m, 4H, H-4, H2-6, OCH_2CH_2OC═O), 3.50 (m, H-2,3,5).

4-Cyano-4-(thiobenzoylthio)pentanoic Acid Chain-Transfer Agent Synthesis. *Bis(thiobenzyl) disulfide (BTBD).* Carbon disulfide (5.25 mL, 87 mmol) was added dropwise to a phenylmagnesium bromide solution in 2-methyl tetrahydrofuran (30 mL, 2.9 M) diluted with tetrahydrofuran (THF) (15 mL) at 0 °C and stirred under argon. The solution was stirred for 45 min and quenched by the dropwise addition of water. The THF was removed in vacuo and the solution was filtered. The product was extracted with DCM as hydrochloric acid was added until the aqueous layer was colorless. The organic layer was washed with brine (2×) and reduced to a red oil in vacuo. The oil was crystallized with ethanol (10 mL), dimethyl sulfoxide (DMSO) (2 mL), and catalytic amounts of crystalline iodine at 0 °C. The magenta crystals were filtered and washed with water (4.18 g, 31%). 1H NMR (300 MHz, CDCl3): δ7.40-8.10 (m, 10H, *ϕ*).

4-Cyano-4-(thiobenzoylthio)pentanoic acid. 4,4′-Azobis(4-cyanovaleric acid) (584 mg, 2.1 mmol) and bis(thiobenzyl) disulfide (425 mg, 1.4 mmol) were dissolved in distilled ethyl acetate (8 mL) and heated to 80 °C for 18 h. The product was isolated as a magenta solid by silica column chromatography using 1:1 ethyl acetate in hexanes as an eluent (470 mg, 60%). ^{1}H NMR (300 MHz, $CDC1_3$): δ7.40-8.00 (m, 5H, *ϕ*), 2.76 (m, CH_2CH_2COOH), 2.45-2.63 (m, CH_2CH_2COOH), 1.96 (s, CH_3).

Reversible Addition-Fragmentation Chain Transfer (RAFT) Polymerization. *Representative Polymerization of Glycomonomer Attached through a Glycosidic Bond.* Glycomonomer (100 equiv.), 4-cyano-4-(thiobenzoylthio)pentanoic acid (1 equiv.), and 4,4′-azobis(4-cyanovaleric acid) (0.3 equiv.) were dissolved in a solution of water/ethanol (3:1). The solution was degassed by five freeze/pump/thaw cycles and heated at 70 °C for 18 h followed by quenching in liquid nitrogen and exposure to air. The reaction was diluted with water, and a sample was lyophilized to determine conversion by ^{1}H NMR. The remainder of the polymer solution was dialyzed in DI water over 16 h, changing the water every 2 h, and lyophilized. The resultant polymer was analyzed by ^{1}H NMR and GPC.

Poly(2-hydroxyethylacrylamide) Synthesis. 2-Hydroxyethylacrylamide (Sigma-Aldrich, 97%, St. Louis, Missouri, USA) was used in place of the glycomonomer following the same procedure as above.

Poly(saccharide acrylate) Self-Assembly. 7.5 nm of titanium followed by 75 nm of gold was evaporated onto a black polystyrene 96-well microtiter plate or a silicon wafer. Wafer pieces were annealed for 1 min with a hydrogen flame before self-assembly. Well plates were visually inspected, and wells that were not fully covered by gold were excluded from the sample. Glycopolymers were dissolved in water at a concentration of 3 mg/mL. 100 μL of ethanolamine was added for each 1 mL of water to the glycopolymer solution. The glycopolymers reacted with the ethanolamine for 30 min before aliquoting 250 μL of solution to each appropriate well on the microtiter plate or 1 mL or more, if applying to pieces of gold-covered wafers. Self-assembly proceeded for 3 days at room temperature. The solution was removed, and the surfaces were rinsed three times with ethanol followed by sterile 137 mM NaCl, 2.7 mM KCl, 10 mM Na_2HPO_4, 1.8 mM KH_2PO_4, (1×) pH 7.2 phosphate-buffered saline (PBS).

11-[(*p*-Phenyl-α-D-Mannopyranosyl)amino-carbonylmethoxyhexa(ethoxy)]undec-1-yl-thiol (Tethered Mannose Monomer) Assembly and Synthesis. Thiol solutions of 0.5 mM 2-(2-[2-(11-mercaptoundecyloxy)-ethoxy]-ethoxy)-ethoxy-acetic acid, 0.5 mM 2-(2-[2-(11-mercaptoundecyloxy)-

https://dx.doi.org/10.1021/acsami.0c04329
ACS Appl. Mater. Interfaces 2020, 12, 35767−35781

ethoxy]-ethoxy)-ethanol, and 130 mM trifluoroacetic acid were mixed and added to the gold surfaces for 3 days. Samples were removed from solution and rinsed with 10% (v/v) triethylamine in ethanol followed by neat ethanol. 0.05 M *N*-hydroxysuccinimide with 0.2 M 1-ethyl-3-(3-dimethylaminopropyl)carbodiimide in water was added to the surfaces for 30 min. The samples were rinsed with water, nitrogen-dried, and added to 2 mg/mL 4-aminophenyl-α-D-mannopyranoside in aqueous 25 mM pH 8.0 sodium phosphate for 2 days. Samples were removed from solution, rinsed with water and ethanol, and then either dried in a nitrogen stream or rinsed with sterile PBS.

X-ray Photoelectron Spectroscopy. An AXIS Ultra DLD X-ray photoelectron spectrometer (Kratos Analytical Inc., Chestnut Ridge, NY, USA) was used for elemental surface analysis. This spectrometer uses a monochromatic Al Kα X-ray source, with a photon energy of 1486.7 eV, with a 200 μm circular spot size and ultrahigh vacuum (10^{-9} torr). Spectra were acquired at a pass energy of 160 eV for survey spectra and 20 eV for high-resolution spectra of C 1s, N 1s, O 1s, S 2p, and Au 4f regions using a 250 ms dwell time. The emission currents were 10 and 20 mA for survey and high-resolution spectra, respectively. 15 kV was the applied electric potential for both scan types. Three scans were performed for survey and Au spectra, 10 scans for N, C, and O spectra, and 15 scans for S spectra.

Bacterial Growth. Lysogeny broth (LB) agar plates containing 50 mg/L kanamycin were used for inoculating liquid cultures. Plates were streaked with *S. oneidensis* MR-1 WT p519nGFP from a −80 °C freezer and incubated for 24 h at 32 °C while shaking at 200 rpm and stored at 4 °C. *S. oneidensis* was precultured by inoculating 20 mL of LB medium in a 125 mL flask and incubating at 32 °C for 24 h of shaking at 200 rpm. 1 mL of the preculture solutions was diluted with 20 mL of LB with 50 mg/L kanamycin. The cultures were incubated until the optical density at 600 nm reached 0.9 typically after about 2 h. The cells were washed by spinning at 2300*g* in a centrifuge for 5 min and then resuspending in PBS. Cells were then spun down and resuspended two more times. The resuspended solutions were diluted 10-fold into PBS and applied to the surface of interest. *S. oneidensis* Δ*msh*A-D was cultured under the same conditions without kanamycin.

Microtiter Plate Fluorescence Measurements. Diluted *S. oneidensis* MR-1 WT p519nGFP culture (250 μL) was aliquoted into each appropriate sample well and incubated at 32 °C for 18 h. For measurement of adhesion without inhibitors, as presented in Figure 3, each well was rinsed three times with 250 μL of PBS and imaged with a fourth addition of 50 μL of PBS.

A Synergy H1 microplate reader was used for surface fluorescent measurements. The excitation was set for 470 nm, and the emission was set for 507 nm. The gain was set to 100. A xenon flash lamp was used as a light source with a 100 ms delay. Ten measurements were used per data point per sample. The read height was 7 mm.

For the experiments measuring the susceptibility of adhered cells to rinses of methyl α-D-mannopyranoside, as shown in Figure 4, the cell culture was prepared and incubated on the surfaces as described above. Then, the culture solution was removed and replaced with 250 μL of 200 mM methyl α-D-mannopyranoside in PBS. The solution was left in the wells as the fluorescence was measured as described above. This measurement constitutes the baseline rinse. The methyl α-D-mannopyranoside solution was incubated on the adhered cells for 5 h before being removed and replaced with another 250 μL of 200 mM methyl α-D-mannopyranoside in PBS. Fluorescence was measured again and recorded as the final rinse.

For the experiments measuring the influence of concurrent incubation with methyl α-D-mannopyranoside, as shown in Figure 5, the cell culture was again prepared as described above. Before adding the cells to the surfaces, 200 mM methyl α-D-mannopyranoside in PBS was added to the appropriate samples to produce a final concentration of 180 mM. Control samples were prepared alongside the methyl α-D-mannopyranoside incubated samples from the same culture and incubated at the same time in PBS. These samples were incubated in their respective solutions for 18 h, as done for the other experiments. The samples were then rinsed one time with 250 μL of PBS for all samples, and the fluorescence was recorded as above.

Glycopolymer Patterning. Silicon wafers covered with 100 nm of gold and a titanium adhesion layer were annealed by a hydrogen flame for 1 min. An AZ nLOF 2020 negative tone photoresist was used to pattern a series of 2 μm lines with a periodicity of 10 μm on the wafers as follows. Wafers were baked at 150 °C for 10 min to dehydrate. They were exposed to hexamethyldisilazane vapors for 15 min. The photoresist was spin-coated at 500 rpm for 5 s and then 3000 rpm for 30 s. Wafers were then soft-baked for 1 min at 110 °C. Total exposure on a Karl Suss contact aligner was 60 mJ. Post-exposure bake was performed for 1 min at 110 °C. Finally, the surfaces were descummed with oxygen plasma at 100 °C for 3 min.

Glycopolymers were self-assembled on the patterned surface as described above for gold-coated wafer pieces. After removing the glycopolymer solution, the samples were rinsed with water and dried with nitrogen. The photoresist was removed by placing the sample in a Baker PRS-3000 photoresist stripper composed of approximately 50% 1-methyl-2-pyrrolidinone, 40% tetrahydrothiophene 1,1-dioxide, and 1-amino-2-propanol. The samples were left in the photoresist stripper for 1 h with gentle heating, then rinsed three times with water, and dried with nitrogen. Poly(2-hydroxyethylacrylamide) (8 mg) was dissolved in 750 μL of water, 200 μL of ethanol, and 50 μL of ethanolamine and was added to the patterned glycopolymer surfaces for 19 h to backfill the gold areas previously covered by the photoresist before stripping. The samples were then rinsed with water and dried with nitrogen.

Application of Bacteria to Glycopolymer Patterns. The molecularly patterned glycopolymer pieces were rinsed with ethanol to sterilize and dried with nitrogen. 5 mL of diluted *S. oneidensis* MR-1 WT p519nGFP in PBS was added to each sample and incubated for 18 h at 32 °C. Cell culture solutions were removed and replaced with 5 mL of fresh PBS. Just before imaging, the samples were rinsed with PBS and placed on a glass coverslip.

An upright ZEISS LSM-800 confocal microscope (Carl Zeiss Microscopy, LLC, White Plains, New York, USA) was used for optical imaging of cells. Green fluorescent protein was excited at 488 nm. Bright field was imaged with confocal reflection at 640 nm and detected at the same wavelength using a photomultiplier tube.

Statistical Analyses. Levels of statistical significance for Figures 3−5 and Figure S1 were determined using unpaired *t* tests. The threshold for significance is a 0.05 *P* value, and values below this threshold are denoted with a single asterisk. Double asterisks indicate *P* values of 0.01−0.001, and triple asterisks indicate *P* values of 0.001 and below.

■ ASSOCIATED CONTENT

Supporting Information

The Supporting Information is available free of charge at https://pubs.acs.org/doi/10.1021/acsami.0c04329.

Additional characterization data and methodology for glycopolymer surfaces (PDF)

■ AUTHOR INFORMATION

Corresponding Author

Paul S. Weiss − *Department of Chemistry & Biochemistry, California NanoSystems Institute, Department of Bioengineering, and Department of Material Science and Engineering, University of California Los Angeles, Los Angeles, California 90095, United States;* orcid.org/0000-0001-5527-6248; Email: psw@cnsi.ucla.edu

Authors

Thomas D. Young − *Department of Chemistry & Biochemistry and California NanoSystems Institute, University of California Los Angeles, Los Angeles, California 90095, United States;* orcid.org/0000-0002-3234-7418

https://dx.doi.org/10.1021/acsami.0c04329
ACS Appl. Mater. Interfaces 2020, 12, 35767−35781

Walter T. Liau − *Department of Bioengineering, University of California Los Angeles, Los Angeles, California 90095, United States*

Calvin K. Lee − *Department of Bioengineering, University of California Los Angeles, Los Angeles, California 90095, United States;* orcid.org/0000-0001-6789-0317

Michael Mellody − *Department of Bioengineering, University of California Los Angeles, Los Angeles, California 90095, United States*

Gerard C. L. Wong − *Department of Chemistry & Biochemistry, California NanoSystems Institute, and Department of Bioengineering, University of California Los Angeles, Los Angeles, California 90095, United States*

Andrea M. Kasko − *Department of Bioengineering and California NanoSystems Institute, University of California Los Angeles, Los Angeles, California 90095, United States;* orcid.org/0000-0003-2355-6258

Complete contact information is available at: https://pubs.acs.org/10.1021/acsami.0c04329

Author Contributions

Experiments were designed by T.D.Y. with input from all authors. Experiments were performed and analyzed by T.D.Y. The glycopolymers were synthesized by W.T.L. The manuscript was written through contributions of all authors. All authors have given approval to the final version of the manuscript.

Notes

The authors declare no competing financial interest.

■ ACKNOWLEDGMENTS

This work was supported by the Office of Naval Research (grant N000141410051) and the Army Research Office (grant W911NF-18-1-0254). We acknowledge the use of the California NanoSystems Institute's facilities: the Advanced Light Microscopy/Spectroscopy Laboratory and the Integrated Nanosystems Cleanroom. We thank Prof. Alvaro Sagasti for the use of his lab's optical microscope and Prof. Kenneth Nealson for his advice and instruction.

■ ABBREVIATIONS

EPS, exopolysaccharide
MSH, mannose-sensitive hemagglutinin
RAFT, reversible addition-fragmentation chain transfer
^{1}H NMR, ^{1}H nuclear magnetic resonance
GPC, gel permeation chromatography
DP_n, degree of polymerization
XPS, X-ray photoelectron spectroscopy
PBS, phosphate-buffered saline
SEM, standard error of the mean
GFP, green fluorescent protein
WT, wild type
DCM, dichloromethane
DI, deionized

■ REFERENCES

(1) Jefferson, K. K. What Drives Bacteria to Produce a Biofilm? *FEMS Microbiol. Lett.* **2004**, *236*, 163−173.
(2) O'Toole, G. A.; Wong, G. C. L. Sensational Biofilms: Surface Sensing in Bacteria. *Curr. Opin. Microbiol.* **2016**, *30*, 139−146.
(3) Lee, C. K.; de Anda, J.; Baker, A. E.; Bennett, R. R.; Luo, Y.; Lee, E. Y.; Keefe, J. A.; Helali, J. S.; Ma, J.; Zhao, K.; Golestanian, R.; O'Toole, G. A.; Wong, G. C. L. Multigenerational Memory and Adaptive Adhesion in Early Bacterial Biofilm Communities. *Proc. Natl. Acad. Sci. U. S. A.* **2018**, *115*, 4471−4476.
(4) Petrova, O. E.; Sauer, K. Sticky Situations: Key Components That Control Bacterial Surface Attachment. *J. Bacteriol.* **2012**, *194*, 2413−2425.
(5) Thormann, K. M.; Saville, R. M.; Shukla, S.; Spormann, A. M. Induction of Rapid Detachment in *Shewanella oneidensis* MR-1 Biofilms. *J. Bacteriol.* **2005**, *187*, 1014−1021.
(6) Li, H.; Opgenorth, P. H.; Wernick, D. G.; Rogers, S.; Wu, T.-Y.; Higashide, W.; Malati, P.; Huo, Y.-X.; Cho, K. M.; Liao, J. C. Integrated Electromicrobial Conversion of CO_2 to Higher Alcohols. *Science* **2012**, *335*, 1596−1596.
(7) Kumar, M.; Morya, R.; Gnansounou, E.; Larroche, C.; Thakur, I. S. Characterization of Carbon Dioxide Concentrating Chemolithotrophic Bacterium Serratia Sp. ISTD04 for Production of Biodiesel. *Bioresour. Technol.* **2017**, *243*, 893−897.
(8) Jiang, X.-R.; Yao, Z.-H.; Chen, G.-Q. Controlling Cell Volume for Efficient PHB Production by *Halomonas*. *Metab. Eng.* **2017**, *44*, 30−37.
(9) Maheshwari, N.; Kumar, M.; Thakur, I. S.; Srivastava, S. Recycling of Carbon Dioxide by Free Air CO_2 Enriched (FACE) *Bacillus* Sp. SS105 for Enhanced Production and Optimization of Biosurfactant. *Bioresour. Technol.* **2017**, *242*, 2−6.
(10) Bond, D. R.; Holmes, D. E.; Tender, L. M.; Lovley, D. R. Electrode-Reducing Microorganisms That Harvest Energy from Marine Sediments. *Science* **2002**, *295*, 483−485.
(11) Ringelberg, D. B.; Foley, K. L.; Reynolds, C. M. Electrogenic Capacity and Community Composition of Anodic Biofilms in Soil-Based Bioelectrochemical Systems. *Appl. Microbiol. Biotechnol.* **2011**, *90*, 1805−1815.
(12) Read, S. T.; Dutta, P.; Bond, P. L.; Keller, J.; Rabaey, K. Initial Development and Structure of Biofilms on Microbial Fuel Cell Anodes. *BMC Microbiol.* **2010**, *10*, 98.
(13) Chen, Q.; Zhu, Z.; Wang, J.; Lopez, A. I.; Li, S.; Kumar, A.; Yu, F.; Chen, H.; Cai, C.; Zhang, L. Probiotic *E. coli* Nissle 1917 Biofilms on Silicone Substrates for Bacterial Interference against Pathogen Colonization. *Acta Biomater.* **2017**, *50*, 353−360.
(14) Biteen, J. S.; Blainey, P. C.; Cardon, Z. G.; Chun, M.; Church, G. M.; Dorrestein, P. C.; Fraser, S. E.; Gilbert, J. A.; Jansson, J. K.; Knight, R.; Miller, J. F.; Ozcan, A.; Prather, K. A.; Quake, S. R.; Ruby, E. G.; Silver, P. A.; Taha, S.; van den Engh, G.; Weiss, P. S.; Wong, G. C. L.; Wright, A. T.; Young, T. D. Tools for the Microbiome: Nano and Beyond. *ACS Nano* **2016**, *10*, 6−37.
(15) Chia, T. W. R.; Nguyen, V. T.; McMeekin, T.; Fegan, N.; Dykes, G. A. Stochasticity of Bacterial Attachment and Its Predictability by the Extended Derjaguin-Landau-Verwey-Overbeek Theory. *Appl. Environ. Microbiol.* **2011**, *77*, 3757−3764.
(16) Felföldi, T.; Jurecska, L.; Vajna, B.; Barkács, K.; Makk, J.; Cebe, G.; Szabó, A.; Záray, G.; Márialigeti, K. Texture and Type of Polymer Fiber Carrier Determine Bacterial Colonization and Biofilm Properties in Wastewater Treatment. *Chem. Eng. J.* **2015**, *264*, 824−834.
(17) Hori, K.; Matsumoto, S. Bacterial Adhesion: From Mechanism to Control. *Biochem. Eng. J.* **2010**, *48*, 424−434.
(18) Terada, A.; Yuasa, A.; Kushimoto, T.; Tsuneda, S.; Katakai, A.; Tamada, M. Bacterial Adhesion to and Viability on Positively Charged Polymer Surfaces. *Microbiology* **2006**, *152*, 3575−3583.
(19) Colville, K.; Tompkins, N.; Rutenberg, A. D.; Jericho, M. H. Effects of Poly(L-Lysine) Substrates on Attached *Escherichia coli* Bacteria. *Langmuir* **2010**, *26*, 2639−2644.
(20) Xia, B.; Shi, J.; Dong, C.; Zhang, W.; Lu, Y.; Guo, P. Covalent Assembly of Poly(Ethyleneimine) via Layer-by-Layer Deposition for Enhancing Surface Density of Protein and Bacteria Attachment. *Appl. Surf. Sci.* **2014**, *292*, 1040−1044.
(21) Thomas, W. Catch Bonds in Adhesion. *Annu. Rev. Biomed. Eng.* **2008**, *10*, 39−57.
(22) Gelimson, A.; Zhao, K.; Lee, C. K.; Kranz, W. T.; Wong, G. C. L.; Golestanian, R. Multicellular Self-Organization of *P. aeruginosa* Due to Interactions with Secreted Trails. *Phys. Rev. Lett.* **2016**, *117*, 178102.

(23) Ma, L.; Lu, H.; Sprinkle, A.; Parsek, M. R.; Wozniak, D. J. *Pseudomonas aeruginosa* Psl Is a Galactose- and Mannose-Rich Exopolysaccharide. *J. Bacteriol.* **2007**, *189*, 8353−8356.
(24) Berne, C.; Ducret, A.; Hardy, G. G.; Brun, Y. V. Adhesins Involved in Attachment to Abiotic Surfaces by Gram-Negative Bacteria. *Microbiol. Spectr.* **2015**, *3*, 163−169.
(25) Firon, N.; Ofek, I.; Sharon, N. Carbohydrate-Binding Sites of the Mannose-Specific Fimbrial Lectins of Enterobacteria. *Infect. Immun.* **1984**, *43*, 1088−1090.
(26) Busch, A.; Waksman, G. Chaperone-Usher Pathways: Diversity and Pilus Assembly Mechanism. *Philos. Trans. R. Soc., B* **2012**, *367*, 1112−1122.
(27) Eshdat, Y.; Ofek, I.; Yashouv-Gan, Y.; Sharon, N.; Mirelman, D. Isolation of a Mannose-Specific Lectin from *Escherichia coli* and Its Role in the Adherence of the Bacteria to Epithelial Cells. *Biochem. Biophys. Res. Commun.* **1978**, *85*, 1551−1559.
(28) Evans, D. J., Jr.; Evans, D. G.; Young, L. S.; Pitt, J. Hemagglutination Typing of *Escherichia coli*: Definition of Seven Hemagglutination Types. *J. Clin. Microbiol.* **1980**, *12*, 235−242.
(29) Qian, X.; Metallo, S. J.; Choi, I. S.; Wu, H.; Liang, M. N.; Whitesides, G. M. Arrays of Self-Assembled Monolayers for Studying Inhibition of Bacterial Adhesion. *Anal. Chem.* **2002**, *74*, 1805−1810.
(30) Fasting, C.; Schalley, C. A.; Weber, M.; Seitz, O.; Hecht, S.; Koksch, B.; Dernedde, J.; Graf, C.; Knapp, E.-W.; Haag, R. Multivalency as a Chemical Organization and Action Principle. *Angew. Chem., Int. Ed.* **2012**, *51*, 10472−10498.
(31) Lundquist, J. J.; Toone, E. J. The Cluster Glycoside Effect. *Chem. Rev.* **2002**, *102*, 555−578.
(32) Sisu, C.; Baron, A. J.; Branderhorst, H. M.; Connell, S. D.; Weijers, C. A. G. M.; de Vries, R.; Hayes, E. D.; Pukin, A. V.; Gilbert, M.; Pieters, R. J.; Zuilhof, H.; Visser, G. M.; Turnbull, W. B. The Influence of Ligand Valency on Aggregation Mechanisms for Inhibiting Bacterial Toxins. *ChemBioChem* **2009**, *10*, 329−337.
(33) Munoz, E. M.; Correa, J.; Riguera, R.; Fernandez-Megia, E. Real-Time Evaluation of Binding Mechanisms in Multivalent Interactions: A Surface Plasmon Resonance Kinetic Approach. *J. Am. Chem. Soc.* **2013**, *135*, 5966−5969.
(34) Barth, K. A.; Coullerez, G.; Nilsson, L. M.; Castelli, R.; Seeberger, P. H.; Vogel, V.; Textor, M. An Engineered Mannoside Presenting Platform: *Escherichia coli* Adhesion under Static and Dynamic Conditions. *Adv. Funct. Mater.* **2008**, *18*, 1459−1469.
(35) Zhu, X.-Y.; Holtz, B.; Wang, Y.; Wang, L.-X.; Orndorff, P. E.; Guo, A. Quantitative Glycomics from Fluidic Glycan Microarrays. *J. Am. Chem. Soc.* **2009**, *131*, 13646−13650.
(36) Song, W.; Xiao, C.; Cui, L.; Tang, Z.; Zhuang, X.; Chen, X. Facile Construction of Functional Biosurface via SI-ATRP and "Click Glycosylation". *Colloids Surf., B* **2012**, *93*, 188−194.
(37) Yu, L.; Hou, Y.; Cheng, C.; Schlaich, C.; Noeske, P.-L. M.; Wei, Q.; Haag, R. High-Antifouling Polymer Brush Coatings on Nonpolar Surfaces via Adsorption-Cross-Linking Strategy. *ACS Appl. Mater. Interfaces* **2017**, *9*, 44281−44292.
(38) Venkateswaran, K.; Moser, D. P.; Dollhopf, M. E.; Lies, D. P.; Saffarini, D. A.; MacGregor, B. J.; Ringelberg, D. B.; White, D. C.; Nishijima, M.; Sano, H.; Burghardt, J.; Stackebrandt, E.; Nealson, K. H. Polyphasic Taxonomy of the Genus *Shewanella* and Description of *Shewanella oneidensis* sp. nov. *Int. J. Syst. Evol. Microbiol.* **1999**, *49*, 705−724.
(39) Fredrickson, J. K.; Romine, M. F.; Beliaev, A. S.; Auchtung, J. M.; Driscoll, M. E.; Gardner, T. S.; Nealson, K. H.; Osterman, A. L.; Pinchuk, G.; Reed, J. L.; Rodionov, D. A.; Rodrigues, J. L. M.; Saffarini, D. A.; Serres, M. H.; Spormann, A. M.; Zhulin, I. B.; Tiedje, J. M. Towards Environmental Systems Biology of *Shewanella*. *Nat. Rev. Microbiol.* **2008**, *6*, 592−603.
(40) Ringeisen, B. R.; Henderson, E.; Wu, P. K.; Pietron, J.; Ray, R.; Little, B.; Biffinger, J. C.; Jones-Meehan, J. M. High Power Density from a Miniature Microbial Fuel Cell Using *Shewanella oneidensis* DSP10. *Environ. Sci. Technol.* **2006**, *40*, 2629−2634.
(41) Xiao, X.; Ma, X.-B.; Yuan, H.; Liu, P.-C.; Lei, Y.-B.; Xu, H.; Du, D.-L.; Sun, J.-F.; Feng, Y.-J. Photocatalytic Properties of Zinc Sulfide Nanocrystals Biofabricated by Metal-Reducing Bacterium *Shewanella oneidensis* MR-1. *J. Hazard. Mater.* **2015**, *288*, 134−139.
(42) Epifanio, M.; Inguva, S.; Kitching, M.; Mosnier, J.-P.; Marsili, E. Effects of Atmospheric Air Plasma Treatment of Graphite and Carbon Felt Electrodes on the Anodic Current from *Shewanella* Attached Cells. *Bioelectrochemistry* **2015**, *106*, 186−193.
(43) Kane, A. L.; Bond, D. R.; Gralnick, J. A. Electrochemical Analysis of *Shewanella oneidensis* Engineered To Bind Gold Electrodes. *ACS Synth. Biol.* **2013**, *2*, 93−101.
(44) Furst, A. L.; Smith, M. J.; Lee, M. C.; Francis, M. B. DNA Hybridization to Interface Current-Producing Cells with Electrode Surfaces. *ACS Cent. Sci.* **2018**, *4*, 880−884.
(45) Saville, R. M.; Dieckmann, N.; Spormann, A. M. Spatiotemporal Activity of the *mshA* Gene System in *Shewanella oneidensis* MR-1 Biofilms. *FEMS Microbiol. Lett.* **2010**, *308*, 76−83.
(46) Utada, A. S.; Bennett, R. R.; Fong, J. C. N.; Gibiansky, M. L.; Yildiz, F. H.; Golestanian, R.; Wong, G. C. L. *Vibrio cholerae* Use Pili and Flagella Synergistically to Effect Motility Switching and Conditional Surface Attachment. *Nat. Commun.* **2014**, *5*, 4913.
(47) Marsh, J. W.; Taylor, R. K. Genetic and Transcriptional Analyses of the *Vibrio cholerae* Mannose-Sensitive Hemagglutinin Type 4 Pilus Gene Locus. *J. Bacteriol.* **1999**, *181*, 1110−1117.
(48) Watnick, P. I.; Fullner, K. J.; Kolter, R. A Role for the Mannose-Sensitive Hemagglutinin in Biofilm Formation by *Vibrio cholerae* El Tor. *J. Bacteriol.* **1999**, *181*, 3606−3609.
(49) Dalisay, D. S.; Webb, J. S.; Scheffel, A.; Svenson, C.; James, S.; Holmstrom, C.; Egan, S.; Kjelleberg, S. A Mannose-Sensitive Haemagglutinin (MSHA)-Like Pilus Promotes Attachment of *Pseudoalteromonas tunicata* Cells to the Surface of the Green Alga *Ulva australis*. *Microbiology* **2006**, *152*, 2875−2883.
(50) Boyd, J. M.; Dacanay, A.; Knickle, L. C.; Touhami, A.; Brown, L. L.; Jericho, M. H.; Johnson, S. C.; Reith, M. Contribution of Type IV Pili to the Virulence of *Aeromonas salmonicida* subsp. *salmonicida* in Atlantic Salmon (*Salmo salar* L.). *Infect. Immun.* **2008**, *76*, 1445−1455.
(51) Jones, C. J.; Utada, A.; Davis, K. R.; Thongsomboon, W.; Zamorano Sanchez, D.; Banakar, V.; Cegelski, L.; Wong, G. C. L.; Yildiz, F. H. C-di-GMP Regulates Motile to Sessile Transition by Modulating MshA Pili Biogenesis and near-Surface Motility Behavior in *Vibrio cholerae*. *PLoS Pathog.* **2015**, *11*, No. e1005068.
(52) Liau, W. T.; Bonduelle, C.; Brochet, M.; Lecommandoux, S.; Kasko, A. M. Synthesis, Characterization, and Biological Interaction of Glyconanoparticles with Controlled Branching. *Biomacromolecules* **2015**, *16*, 284−294.
(53) Fais, M.; Karamanska, R.; Allman, S.; Fairhurst, S. A.; Innocenti, P.; Fairbanks, A. J.; Donohoe, T. J.; Davis, B. G.; Russell, D. A.; Field, R. A. Surface Plasmon Resonance Imaging of Glycoarrays Identifies Novel and Unnatural Carbohydrate-Based Ligands for Potential Ricin Sensor Development. *Chem. Sci.* **2011**, *2*, 1952−1959.
(54) Lowe, S.; O'Brien-Simpson, N. M.; Connal, L. A. Antibiofouling Polymer Interfaces: Poly(ethylene glycol) and Other Promising Candidates. *Polym. Chem.* **2015**, *6*, 198−212.
(55) Zheng, X.; Zhang, C.; Bai, L.; Liu, S.; Tan, L.; Wang, Y. Antifouling Property of Monothiol-Terminated Bottle-Brush Poly(methylacrylic acid)-graft-poly(2-methyl-2-oxazoline) Copolymer on Gold Surfaces. *J. Mater. Chem. B* **2015**, *3*, 1921−1930.
(56) Biggs, C. I.; Walker, M.; Gibson, M. I. "Grafting to" of RAFTed Responsive Polymers to Glass Substrates by Thiol−Ene and Critical Comparison to Thiol−Gold Coupling. *Biomacromolecules* **2016**, *17*, 2626−2633.
(57) Weck, M.; Jackiw, J. J.; Rossi, R. R.; Weiss, P. S.; Grubbs, R. H. Ring-Opening Metathesis Polymerization from Surfaces. *J. Am. Chem. Soc.* **1999**, *121*, 4088−4089.
(58) Coullerez, G.; Gorodyska, G.; Reimhult, E.; Textor, M.; Grandin, H. M. Self-Assembled Multifunctional Polymers for Biointerfaces. In *Functional Polymer Films*; Knoll, W., Advincula, R. C., Eds.; Wiley-VCH Verlag GmbH & Co. KgaA: Weinheim, Germany, 2011; *2*, 859−863.

https://dx.doi.org/10.1021/acsami.0c04329
ACS Appl. Mater. Interfaces 2020, 12, 35767−35781

(59) Wang, Y.; Narain, R.; Liu, Y. Study of Bacterial Adhesion on Different Glycopolymer Surfaces by Quartz Crystal Microbalance with Dissipation. *Langmuir* **2014**, *30*, 7377−7387.
(60) Chiefari, J.; Chong, Y. K.; Ercole, F.; Krstina, J.; Jeffery, J.; Le, T. P. T.; Mayadunne, R. T. A.; Meijs, G. F.; Moad, C. L.; Moad, G.; Rizzardo, E.; Thang, S. H. Living Free-Radical Polymerization by Reversible Addition−Fragmentation Chain Transfer: The RAFT Process. *Macromolecules* **1998**, *31*, 5559−5562.
(61) Dumas, C.; Basseguy, R.; Bergel, A. Electrochemical Activity of *Geobacter sulfurreducens* Biofilms on Stainless Steel Anodes. *Electrochim. Acta* **2008**, *53*, 5235−5241.
(62) Zhou, M.; Chi, M.; Luo, J.; He, H.; Jin, T. An Overview of Electrode Materials in Microbial Fuel Cells. *J. Power Sources* **2011**, *196*, 4427−4435.
(63) He, Y.-R.; Xiao, X.; Li, W.-W.; Sheng, G.-P.; Yan, F.-F.; Yu, H.-Q.; Yuan, H.; Wu, L.-J. Enhanced Electricity Production from Microbial Fuel Cells with Plasma-Modified Carbon Paper Anode. *Phys. Chem. Chem. Phys.* **2012**, *14*, 9966−9971.
(64) Zhang, T.; Nie, H.; Bain, T. S.; Lu, H.; Cui, M.; Snoeyenbos-West, O. L.; Franks, A. E.; Nevin, K. P.; Russell, T. P.; Lovley, D. R. Improved Cathode Materials for Microbial Electrosynthesis. *Energy Environ. Sci.* **2013**, *6*, 217−224.
(65) Baudler, A.; Schmidt, I.; Langner, M.; Greiner, A.; Schröder, U. Does It Have to Be Carbon? Metal Anodes in Microbial Fuel Cells and Related Bioelectrochemical Systems. *Energy Environ. Sci.* **2015**, *8*, 2048−2055.
(66) Aryal, N.; Ammam, F.; Patil, S. A.; Pant, D. An Overview of Cathode Materials for Microbial Electrosynthesis of Chemicals from Carbon Dioxide. *Green Chem.* **2017**, *19*, 5748−5760.
(67) Shuster, M. J.; Vaish, A.; Szapacs, M. E.; Anderson, M. E.; Weiss, P. S.; Andrews, A. M. Biospecific Recognition of Tethered Small Molecules Diluted in Self-Assembled Monolayers. *Adv. Mater.* **2008**, *20*, 164−167.
(68) Shuster, M. J.; Vaish, A.; Gilbert, M. L.; Martinez-Rivera, M.; Nezarati, R. M.; Weiss, P. S.; Andrews, A. M. Comparison of Oligo(ethylene glycol)alkanethiols versus *n*-Alkanethiols: Self-Assembly, Insertion, and Functionalization. *J. Phys. Chem. C* **2011**, *115*, 24778−24787.
(69) Li, X.; Lin, J.; Qiu, Y. Influence of He/O_2 Atmospheric Pressure Plasma Jet Treatment on Subsequent Wet Desizing of Polyacrylate on PET Fabrics. *Appl. Surf. Sci.* **2012**, *258*, 2332−2338.
(70) Levan, S.; De, S.; Olson, R. *Vibrio cholerae* Cytolysin Recognizes the Heptasaccharide Core of Complex N-Glycans with Nanomolar Affinity. *J. Mol. Biol.* **2013**, *425*, 944−957.
(71) Fong, J. N. C.; Yildiz, F. H. Biofilm Matrix Proteins. *Microbiol. Spectr.* **2015**, *3*, 201−222.
(72) Teschler, J. K.; Zamorano-Sánchez, D.; Utada, A. S.; Warner, C. J. A.; Wong, G. C. L.; Linington, R. G.; Yildiz, F. H. Living in the Matrix: Assembly and Control of *Vibrio cholerae* Biofilms. *Nat. Rev. Microbiol.* **2015**, *13*, 255−268.
(73) Pranantyo, D.; Xu, L. Q.; Hou, Z.; Kang, E.-T.; Chan-Park, M. B. Increasing Bacterial Affinity and Cytocompatibility with Four-Arm Star Glycopolymers and Antimicrobial α-Polylysine. *Polym. Chem.* **2017**, *8*, 3364−3373.
(74) Yu, K.; Creagh, A. L.; Haynes, C. A.; Kizhakkedathu, J. N. Lectin Interactions on Surface-Grafted Glycostructures: Influence of the Spatial Distribution of Carbohydrates on the Binding Kinetics and Rupture Forces. *Anal. Chem.* **2013**, *85*, 7786−7793.

https://dx.doi.org/10.1021/acsami.0c04329
ACS Appl. Mater. Interfaces 2020, 12, 35767−35781